transfection efficiency was normalized relative to the β-galactosidase activity (See Materials and Methods). **D**, Schematic representation of a series of deletion mutants of the DKK2 5′ upstream region. KpnI (−1741), NheI (−1241) and SacI (−521) sites were used to construct a series of deletion mutants of the DKK2 promoter (see Materials and Methods). **E**, **F**, **G**, The transactivation of deletion mutants of the DKK2 promoter by EWS/ETS expression. HEK293 cells were co-transfected with reporter plasmids and the expression vector. Data are normalized to the value for the empty vector (pcDNA3-flagDEST) which is arbitrarily set to 1. Luciferase activity was measured after 48 hours. Data are relative values with the SD for triplicate wells. The transfection efficiency was normalized relative to the β-galactosidase activity (See Materials and Methods).
doi:10.1371/journal.pone.0004634.g002

PCR and cloned into the *Xmn*I-*EcoR*V sites of pENTR^{TM}11 (Invitrogen). The resulting pENTR11-EWS/ETSs were recombined with pcDNA3-flagDEST using the LR recombination reaction as instructed by the manufacturer (Invitrogen) to construct the flag-tagged EWS/ETS expression vector pcDNA3-flagEWS/ETSs. The human DKK1 and DKK2 cDNAs without a stopcodon were subcloned into pENTR^{TM}11 and the resulting pENTR11-DKK1 and pENTR11-DKK2 were recombined with pcDNA-DEST40 C-terminally V5-His-tagged (Invitrogen) using the LR recombination reaction as instructed by the manufacturer, to obtain pcDNA-DEST40-DKK1 and -DKK2.

Cell cultures

H4-1 (primary hMPCs), UEET-12, UET-13 (hMPCs with an extended life span through retroviral transduction) [39] and UET-13 transfectants [35] were cultured in Dulbecco's modified Eagle's medium (DMEM) with 10% Fetal Bovine Serum (FBS) or Tet System Approved FBS (Takara) at 37°C under a humidified 5%

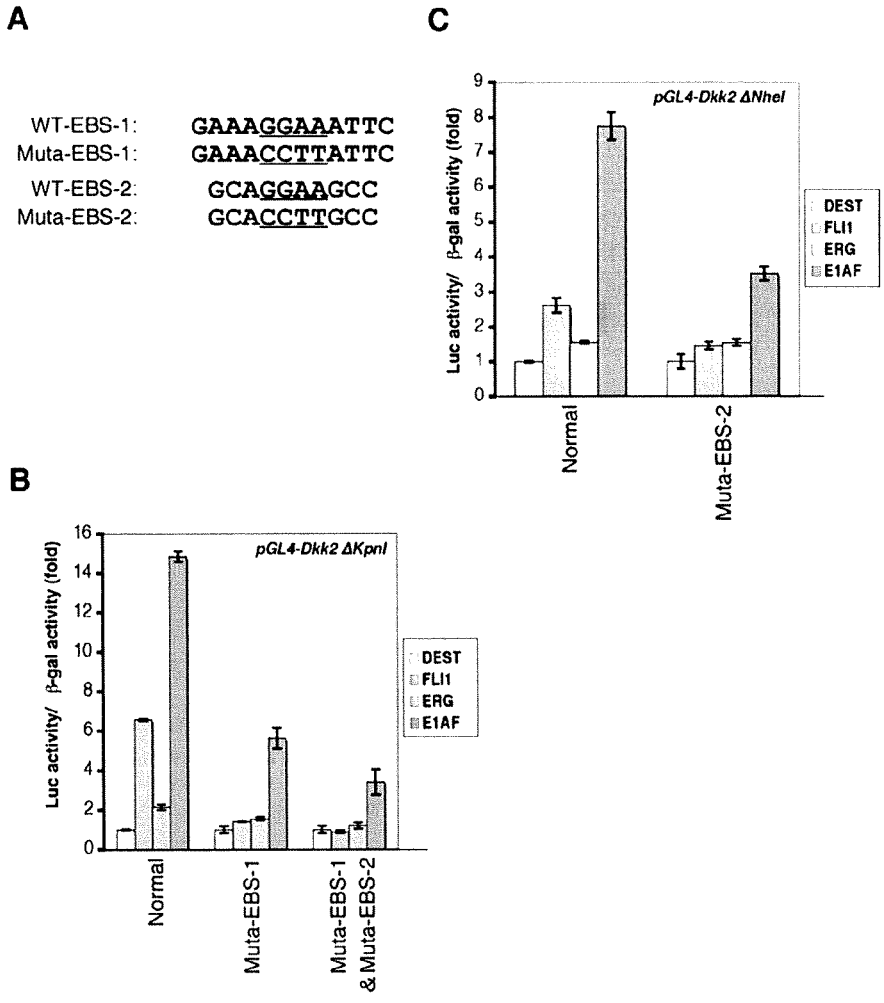

Figure 3. Mutational analysis of EBS in the DKK2 promoter. **A**, The substitutions in EBS-1 and EBS-2. The underlined sequences indicate the mutated sequences in EBS. **B**, **C**, The suppression of EWS/ETS-mediated activation of the DKK2 promoter by the mutations. HEK293 cells were co-transfected with mutated reporter plasmids and the expression vector. Luciferase activity was measured after 48 hours. Data are relative values with the SD for triplicate wells. Data are normalized to the value for the empty vector (pcDNA3-flagDEST) that is arbitrarily set to 1. The transfection efficiency was normalized relative to the β-galactosidase activity (See Materials and Methods).
doi:10.1371/journal.pone.0004634.g003

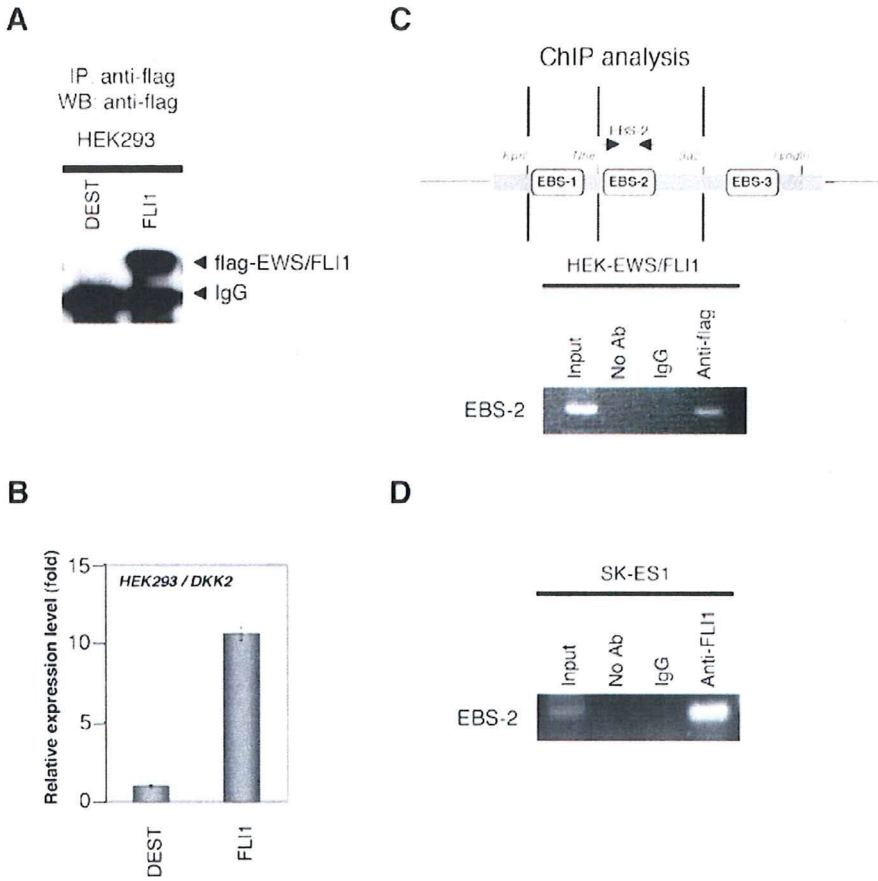

Figure 4. Direct binding of EWS/FLI1 to EBS of the DKK2 promoter. A, Immunoprecipitation (IP) and Western blot analysis of HEK293 cells stably transfected with pcDNA3-flagDEST (HEK-DEST) or pcDNA3-flagEWS/FLI1 (HEK-EWS/FLI1). Cells were lysed and Immunoprecipitated by anti-flag antibodies. The IP products were analyzed by Westen blot analysis. **B,** Real-time RT-PCR analysis using HEK293 transfectants for DKK2 expression. Data are normalized to the mRNA level in HEK-DEST cells which is arbitrarily set to 1. Signal intensity was normalized using that of a control housekeeping gene (human GAPDH gene). Data are relative values with the SD for triplicate wells. DEST: HEK-DEST cells; FLI1: HEK-EWS/FLI1. **C, D,** Binding of EWS/FLI1 to EBS of the DKK2 promoter *in vivo*. The ChIP analysis was done as described under Materials and Methods. For the ChIP analysis using HEK293 transfectants, soluble chromatin was immunoprecipitated with anti-flag antibodies or normal mouse immunoglobulin (IgG) and analyzed by PCR. For the ChIP analysis using SK-ES1 cells, soluble chromatin was immunoprecipitated with anti-FLI1 antibodies or normal rabbit immunoglobulin (IgG) and analyzed by PCR. The upper figure indicates a schematic representation of the site of the DKK2 promoter detected in the ChIP analysis. Arrows indicate the position of the specific primer used for ChIP.
doi:10.1371/journal.pone.0004634.g004

CO_2 atmosphere. The EFT cell lines EES-1, SCCH196, RD-ES, SK-ES1, NCR-EW2, NCR-EW3 and W-ES, neuroblastoma (NB) cell lines NB9, NB69 and GOTO, and Rhabdomyosarcoma (RMS) cell line NRS-1 were maintained as described previously [35]. Other NB cell lines NB1, NB19 [40], CHP134 and IMR32 [41], the Burkitt lymphoma (BL) cell lines BJAB, Ramos, Daudi, P3HR1 and Raji (obtained from Japanese Collection of Research Bioresources, JCRB, Osaka, Japan) were cultured in RPMI 1640 medium with 10% FBS. Embryonal carcinoma (EC) cell lines NCR-G2 and NCR-G3 [42] were cultured in a 1:1 mixture of DMEM and Ham's F12 medium with 10% FBS.

HEK293 cells were cultured in DMEM with 10% FBS. Stable transfection of HEK293 cells with pcDNA3-flagDEST or pcDNA3-flagEWS/FLI1 was performed using Lipofectamine^{TM} 2000 (Invitrogen) according to the manufacturer's directions. Individual resistant clones were selected in the presence of 1000 μg/ml of G418 for a month and designated as HEK-DEST and HEK-EWS/FLI1 cells.

For the generation of SK-ES1 transfectants with DKK1 and DKK2, SK-ES1 cells transfected with pcDNA-DEST40-DKK1 and -DKK2, respectively and selected as described above. The consequent stable transfectants were designated SK-ES1-DKK1 and -DKK2, respectively. As a negative control, SK-ES1 cells were also transfected with empty vector pcDNA-DEST40 and designated as SK-ES1-DEST.

Western blot analysis

The Western blot analysis was performed as described [43]. Briefly, cell lysate was prepared, separated on a 10% SDS-PAGE gel, and transferred onto a PVDF membrane. After blocking with 5% skim milk in PBS containing 0.01% Tween-20 (Sigma) (PBST), the membrane was incubated with appropriate primary and secondary antibodies. As the primary antibody, anti-flag M2 (Sigma), anti-V5 (Invitrogen) or anti-Actin (Sigma) was used. HRP-conjugated anti-rabbit or anti-mouse IgG antibody (Dako-Cytomation) was used as the secondary antibody. Blots were

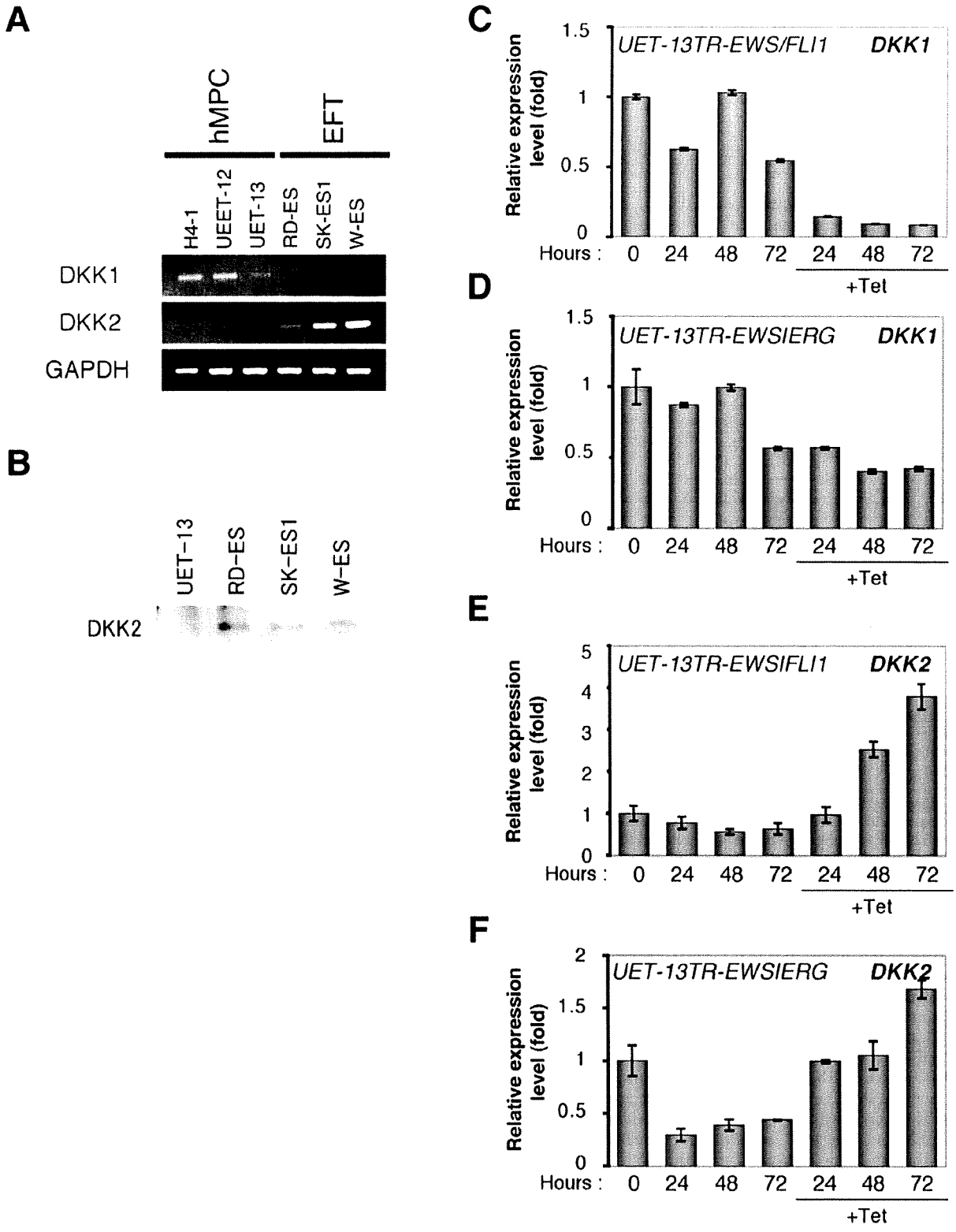

Figure 5. The change in expression pattern of the DKK family with EWS/ETS's induction in UET-13 cells. A, The expression pattern of DKKs in hMPCs and EFT cells. DKK1 and DKK2 mRNAs in the H4-1, UEET-12, UET-13 and EFT cell lines were detected by RT-PCR. As an internal control, a human GAPDH gene was used. **B**, The expression of DKK2 protein in hMPCs and EFT cells. For the detection of secreted DKK2, cells were cultured

for 48 hours and then the culture medium was analyzed by Western blotting. **C, D, E, F,** Relative level of DKK1 (**C, D**) and DKK2 (**E, F**) in UET-13 transfectants in the absence or presence of tetracycline. UET-13 transfectants were treated with or without 3 μg/ml of tetracycline for the indicated periods. Real-time RT-PCR was performed to investigate the expression pattern of the DKK family. Signal intensity was normalized using that of a control housekeeping gene (human GAPDH gene). Data are relative values with the SD for triplicate wells and normalized to the mRNA level at 0 hour which is arbitrarily set to 1.
doi:10.1371/journal.pone.0004634.g005

detected using an ECL Plus Western Blotting Detection System (GE Healthcare Bio-Science Corp) and exposed to X-ray film (Kodak) for 5–30 minutes. Secreted DKK2 was detected using anti-DKK2 antibody (Biovision). For the detection of secreted DKKs-V5 proteins, 20 ml of each cell culture supernatant in SK-ES1 transfectants was collected and added to BD TALON Metal Affinity Resin (Clontech). After incubation overnight, the supernatant was removed. The resin-protein complex was purified and analyzed by Western blotting as described above.

Immunoprecipitation (IP)

IP was performed as described previously [44]. Whole cell extracts were incubated with anti-flag M2 antibody (Sigma) and the protein-antibody complex was bound to protein G-Dynal beads (Invitrogen). The bound complexes were washed and collected by centrifugation and separated by SDS-PAGE.

Reporter assay

HEK293 cells were transiently transfected with a mixture of 100 ng of pGL4 or the pGL4-DKK2 reporter vector series and 300 ng of pcDNA3-flagDEST or pcDNA3-flagEWS/ETS using Lipofectamine™ 2000 (Invitrogen). The cells were also transfected with 25 ng of pcDNA/GW-40/LacZ (Invitrogen) for the standardization of transfection efficiency. The luciferase activity and β-gal activity were measured 48 h after the transfection as described before (Mon *et al.*, 2003).

RT-PCR analysis

RT-PCR analysis was performed as described [35]. Total RNA was extracted from cells using a RNeasy kit (QIAGEN) and reverse transcribed using a First-Strand cDNA Synthesis Kit (GE Healthcare Bio-Science Corp). The primers used for the detection of DKK1 and DKK2 were as follows: DKK1 primers, 5′-CGCTAGTCCC ACCCGCGGAG GGGACGCAGG -3′ and 5′-CCTTCTTTCA GGACAGGTTT ACAGATCTTG -3′; DKK2 primers, 5′-GAAGCGCTGC CACCGAGATG GCATGTGCTG -3′ and 5′-GATGATCGTA GGCAGGGGTC TCCTTCATGC -3′). For the detection of DKK-V5 fusion transcripts, the following V5-specific primer was used: V5 (reverse): 5′-ACGCGTAGAATCGAGACC-GAGAGAGGGTT-3′. The human GAPDH gene was detected as an internal control with the following primers: GAPDH (forward): 5′-CCACCCATGG CAAATTCCAT GGCA-3′, GAPDH (reverse): 5′-TCTAGACGGC AGGTCAGGT CCACC-3′. PCR products were electrophoresed with a 1% agarose gel and stained by ethidium bromide.

Real-time RT-PCR analysis

Real-time RT-PCR was performed using SYBR® Green PCR Master Mix, TaqMan® Universal PCR Master Mix and TaqMan® Gene Expression Assays, Inventoried assay on an ABI PRISM® 7900HT Sequence Detection System (Applied Biosystems) according to the manufacturer's instructions. The human GAPDH gene was used as an internal control for normalization.

Subcutaneous tumorigenicity assay

Immuno-deficient mice (CB17-SCID 8 weeks old, Clea Japan, Inc) were maintained under pathogen-free conditions. SK-ES1 transfectants were suspended in 100 μl of PBS and injected s.c. into mice. Cells were injected at a density of 1×10^7 cells per body. Mice were monitored weekly and tumor diameter was measured with precision calipers. Mice were sacrificed after 28 days of monitoring.

Chromatin immunoprecipitation (ChIP) assay

For preparing the antibody- protein G-Dynal beads (Invitrogen) complex, protein G-Dynal beads were washed with 0.5% BSA in PBS, and anti-flag antibody, anti-FLI1 antibody (Santa cruz) or mouse IgG was added. The beads mixtures were incubated and rotated overnight at 4°C. HEK-EWS/FLI1 cells or SK-ES1 cells were cross-linked by 1% formaldehyde for 10 minutes at room temperature. The medium was aspirated and the cells were lysed using cell lysis buffer A [50 mM HEPES pH 7.5, 140 mM NaCl, 1 mM EDTA, 10% glycerol, 0.5% NP-40, 0.25% Triton X-100, and Complete protease inhibitor cocktail (Roche)]. The cells were pelleted and resuspended in cell lysis buffer B [10 mM Tris-HCl pH 8.0, 200 mM NaCl, 1 mM EDTA, 0.5 mM EGTA, and Complete protease inhibitor cocktail]. Nuclei were then pelleted and lysed with cell lysis buffer C [10 mM Tris-Hcl pH 8.0, 100 mM NaCl, 1 mM EDTA, 0.5 mM EGTA, 0.1% deoxycholate, 0.5% N-lauroylsarcosine, Complete protease inhibitor cocktail] on ice. The nuclear lysates were sonicated and then precleared with salmon sperm DNA/ protein G-Dynal beads for 3 hours. The cleared supernatant was incubated with anti-flag antibody, anti-FLI1 antibody or mouse IgG- protein G-Dynal beads complex. Sixteen hours after the incubation, the immune complexes were collected with centrifugation and washed 7 times using RIPA buffer [50 mM HEPES pH 7.5, 500 mM LiCl, 1 mM EDTA, 1% NP-40, 0.7% N-lauroylsarcosine, and Complete protease inhibitor cocktail]. The DNA-protein cross-linking was reversed by heating at 65°C. The chromatin was purified and analyzed by PCR using specific primers (EBS-2: 5′-GCAG-GAAGCC AAGGAAGACA-3′ and 5′-GCGAATAGGA AATCCCAGAT AGG-3′). PCR products were electrophoresed with a 2% agarose gel and stained by SYBR® Green I (Takara).

Results

Increased DKK2 and suppressed DKK1 expression in EFT cells

To identify the specific genes related to EFT cells, DNA microarray-based global expression profiling was done using EFT cell lines and other tumors found in children. By comparing the expression patterns, genes were identified as typically up-regulated in EFT cells and other cells (data not shown). Among these genes, we particularly focused on DKK2 (up-regulated) and DKK1 (down-regulated) because they are members of the DKK family and structurally well related, but revealed opposite expression patterns in EFT cells. Similar results were obtained from the microarray assay using EFT and NB tissue samples in the Gene

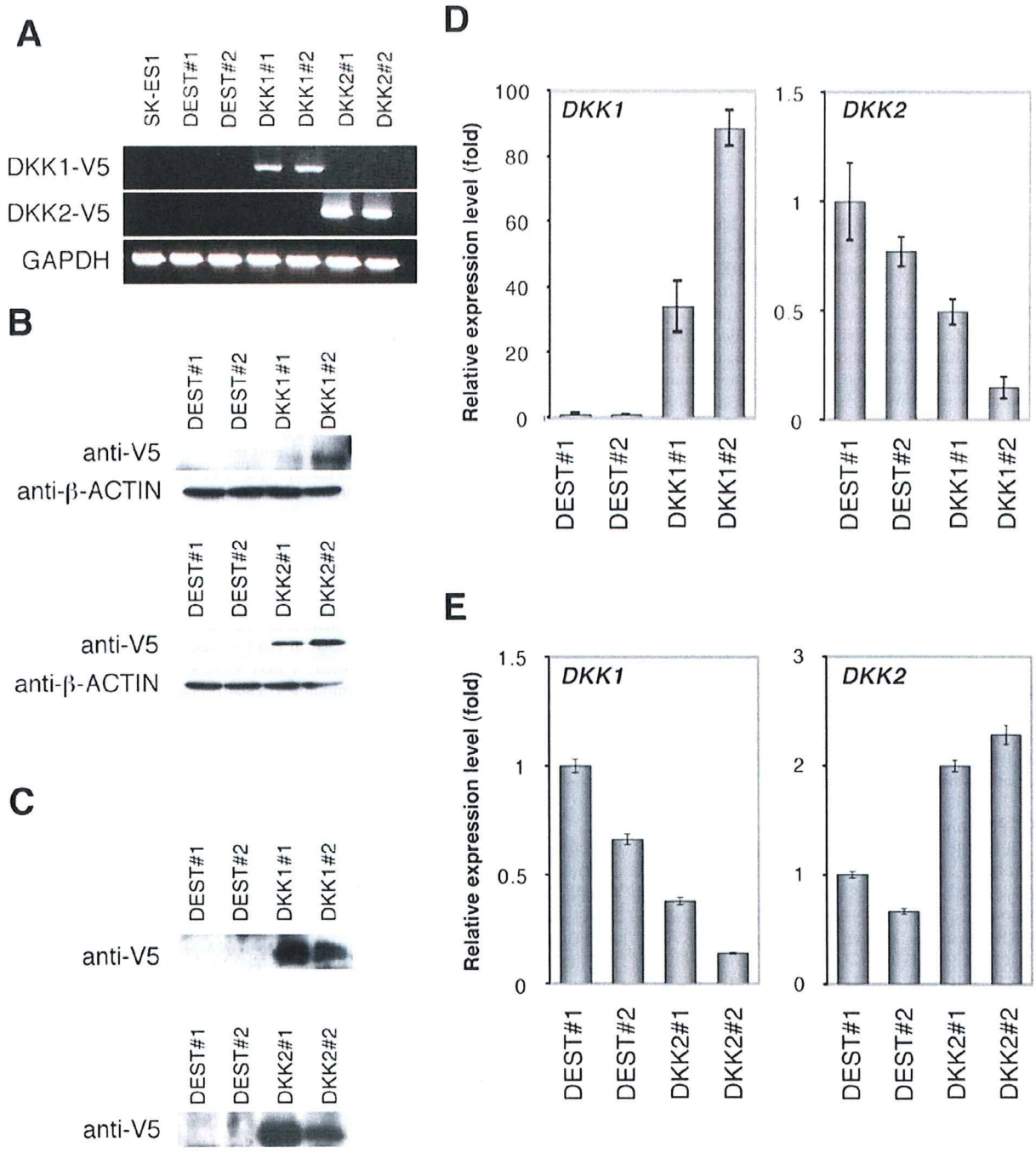

Figure 6. Mutually exclusive expression of DKK1 and DKK2 in SK-ES1 cells. A, B, Validation of DKK-V5 expression in SK-ES1 cells. The expression of DKK1-V5 and DKK2-V5 in SK-ES1 transfectants was observed by RT-PCR (**A**) and Western blot analysis (**B**). DEST#1, #2: SK-ES1-DEST#1, #2, DKK1#1, #2: SK-ES1-DKK1#1, #2, DKK2#1, #2: SK-ES1-DKK2#1, #2. As an internal control, human GAPDH (for RT-PCR) and β-Actin (for Western blot) were used, respectively. **C,** Secretion of DKKs-V5 into cell culture supernatants. Secreted DKKs-V5 proteins were absorbed by TALON Metal Affinity Resin (Clontech) and analyzed by Western blotting, **D, E,** Relative level of DKK1 and DKK2 in SK-ES1 transfectants in SK-ES1-DKK1 (**D**) and SK-ES1-DKK2 (**E**). Signal intensity was normalized using that of a control housekeeping gene (human GAPDH gene). Data are relative values with the SD for triplicate wells and normalized to the mRNA level at DEST#1 which is arbitrarily set to 1.
doi:10.1371/journal.pone.0004634.g006

Expression Omnibus database GEO (Accession number: GSE1825) (data not shown).

We first confirmed the expression pattern of DKK genes obtained with the microarray assay by conducting a Real-time RT-PCR analysis. The increased expression of DKK2 was confirmed in EFT cells (Fig. 1A). DKK2 expression was especially increased in NCR-EW3 cells that express EWS/E1AF. In contrast, the expression of DKK1 was suppressed in most EFT cells (Fig. 1B).

Direct regulation of DKK2, but not DKK1, promoter activity by EWS/ETS proteins

Previous reports revealed that EWS/ETS proteins enhance the promoter activity of several genes via the ets DNA-binding sites on the promoters [45]. A sequence analysis and TF search (http://www.cbrc.jp/ research/db/TFSEARCH.html) revealed the 5′ upstream region (−1955 to +49) of the DKK2 gene to have two putative EBSs, here designated EBS-1 (−1585 to −1573) and EBS-2 (−904 to −895). Although, the TF search did not recognize it, we also found a putative EBS (GGAA/T) element, designated as EBS-3 (−140 to −131). Thus, we next isolated the 5′ upstream region of the DKK2 gene and cloned it into the reporter plasmid pGL4 (DKK2 full-Luc) (Fig. 2A) to test the effects of EWS/ETS expression on DKK2 promoter activity with transient transfection reporter assays in HEK293 cells. As shown in Fig. 2B and C, co-transfection of EWS/ETS with pGL4-DKK2 resulted in an enhancement of reporter activity ~10-fold compared with co-transfection with empty expression vector. To map the site in the DKK2 5′ upstream region required for activation by EWS/ETS expression, reporter assays using a deletion series of pGL4-DKK2 were performed. Co-transfection of the EWS/ETS expression vector with DKK2 pGL4-DKK2Δ*Kpn*I or -DKK2Δ*Nhe*I resulted in a strong induction of the reporter activity (~15-fold) (Fig. 2D–F), whereas that with pGL4-DKK2Δ*Sac*I led to only a faint enhancement (Fig. 2G), indicating that the sequence from -521 to +49 in the DKK2 gene is not sufficient for EWS/ETS-mediated enhancement of DKK2 transcription.

To determine whether the EBSs are involved in the EWS/ETS-induced transactivation of the DKK2 promoter activity, effects of mutagenesis of EBS-1 and EBS-2 were tested. As shown in Fig. 3A and 3B, the mutation of EBS-1 suppressed the EWS/ETS-induced enhancement of the reporter activity of DKK2Δ*Kpn*I. When both EBS-1 and EBS-2 were simultaneously mutated, the suppressive effect against EWS/ETS was further strengthened (Fig. 3B). Likewise, the mutation of EBS-2 suppressed the EWS/ETS-induced activation of the reporter activity of DKK2 Δ*Nhe*I-Luc (Fig. 3A, C).

We next evaluated the direct binding of EWS/ETS proteins to the EBSs in the DKK2 5′ upstream region. In this assay, HEK293 cells were stably transfected with pcDNA-flagDEST and pcDNA-flagEWS/FLI1, respectively. The overexpression of flag-tagged EWS/FLI1 protein was confirmed in the IP-western blot assay (Fig. 4A). DKK2 expression was significantly up-regulated in HEK-EWS/FLI1 transfectants, approximately 10 fold, compared with HEK-DEST cells (Fig. 4B). When the ChIP assay was performed using these cells as illustrated in Fig. 4C (upper figure), we found that EWS/FLI1 preferentially bound to EBS-2 in HEK-EWS/FLI1 transfectants (Fig. 4C). Similarly, we also demonstrated that EWS/FLI1 bound to EBS-2 in SK-ES1 cells (Fig. 4D).

We also examined the effects of EWS/ETS expression on DKK1 promoter activity. Although we also isolated the 5′ upstream region of the DKK1 gene (−2108/+80) and conducted reporter assays as for the DKK2 gene, no significant enhancement of DKK1 promoter activity mediated by EWS/ETS expression was observed (data not shown).

Alteration of DKK1 and DKK2 expression by EWS/ETS in human MPCs

Although the origin of EFT is still unknown, some experimental results point to hMPCs. In hMPCs, DKK1 has a crucial role in proliferation and osteogenic differentiation [46,47]. As shown in Fig. 5A, DKK1, but not DKK2, was expressed in primary hMPCs, H4-1 cells, UEET-12 cells and UET-13 cells. The expression of DKK2 protein was also confirmed in EFT whereas not in UET-13 cells (Fig. 5B). In EFT cell lines, by contrast, DKK2, but not DKK1, was expressed. We previously reported that the tetracycline-dependent expression of EWS/ETS confers EFT-like phenotypes in UET-13 cells [35]. Therefore, we tested the change of DKK gene expression using this model. As shown in Fig. 5C–F, both EWS/FLI1 and EWS/ERG expression resulted in a considerable increase in DKK2 gene expression. It is worth noting to describe that the expression level of the DKK1 gene was significantly decreased after EWS/ETS expression in UET-13 cells.

Mutually exclusive expression of DKK1 and DKK2 in SK-ES1 cells

To further elucidate the biological roles of DKK genes in EFT cells, we introduced the DKK1 and DKK2 genes into the EFT cell line SK-ES1, in which the level of DKK2 expression is relatively low (Fig. 1A). Independent transfectants were confirmed to indeed express each gene by RT-PCR and Western blotting (Fig. 6A–C). Interestingly, when the DKK1 transfectants were examined by real-time PCR analysis, a reduction in DKK2 expression was found (Fig. 6D). In contrast, DKK2 overexpression induced a reduction in DKK1 expression in SK-ES1 cells (Fig. 6E). These results suggested that the expression of DKK1 and DKK2 related reciprocally in a mutually exclusive fashion in SK-ES1 cells.

Expression of DKK1 inhibits the formation of subcutaneous tumors

We next investigated the effect of DKK1 and DKK2 expression on tumorigenicity by subcutaneously implanting SK-ES1 transfectants into CB17/SCID mice. SK-ES1-DEST#1 and SK-ES1-DKK1#1 were implanted subcutaneously into CB17/SCID mice. The mice were sacrificed 28 days after injection. Four of the 10 mice injected with SK-ES1-DEST cells developed tumors (experiment #1 in Table. 1, Fig. 7A), in the case of SK-ES1-DKK1#1 cells, however, only one tumor mass was observed after similar preparation. In addition, the xenograft of DKK1-expressing SK-ES1 cells was significantly smaller than that of control SK-ES1-DEST cells (Fig. 7A, B). There were no morphological and pathological differences between xenografts formed by SK-ES1-DEST#1 and -DKK1#1 cells. Reproducible results were obtained by using another independent clone, SK-ES-DKK1#2 cells (experiment #2 in Table. 1). We also tested the tumorigenicity of SK-ES1-DKK2 cells in a similar manner.

Table 1. Formation of subcutaneous tumors in CB17/SCID mice by SK-ES1 cells.

Cells	Number tumors/ number injected	
	Experiments#1	Experiments#2
DEST	4/10	5/5
DKK1	1/10	2/5

doi:10.1371/journal.pone.0004634.t001

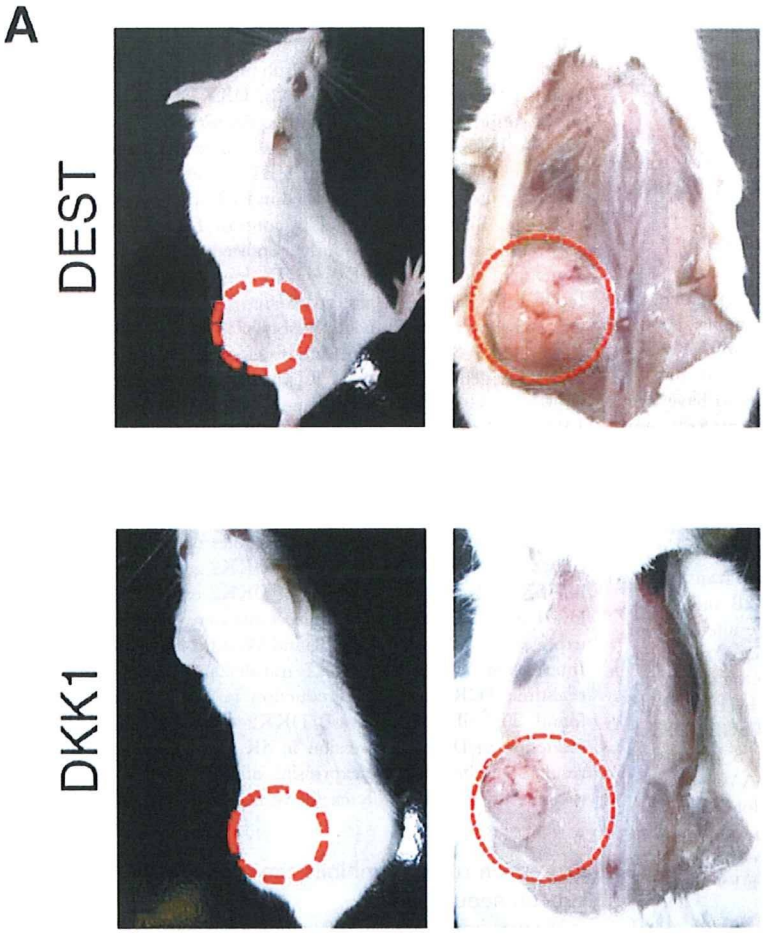
A
DEST
DKK1

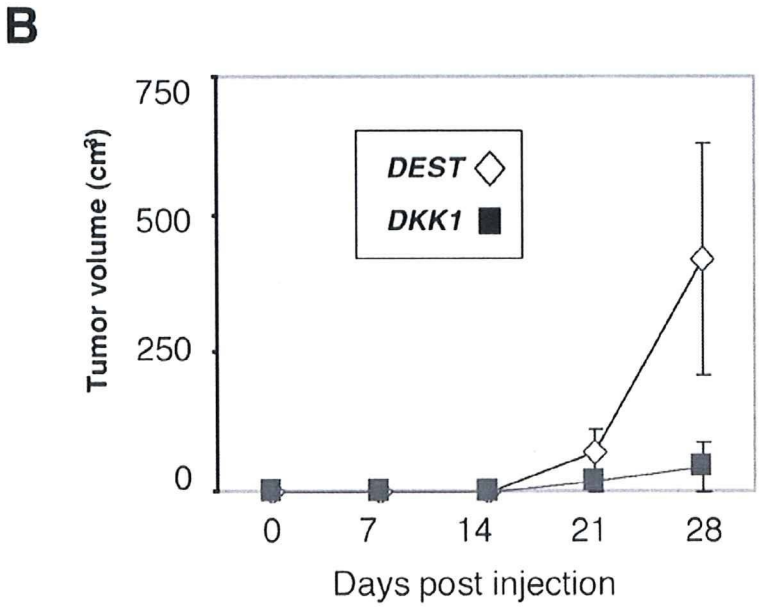
B
Tumor volume (cm³)
750
500
250
0
DEST
DKK1
0
7
14
21
28
Days post injection

Figure 7. The effect of ectopic DKK1 expression on tumor cell growth *in vivo*. **A**, Examples of Immuno-deficient mice that have been injected with SK-ES1-DEST (DEST#1) and SK-ES1-DKK1 (DKK1#1) (left panels). The image was taken at 28 days after injection. Right panels indicate the xenografts of mice injected with DEST#1 and DKK1#1. Red circles indicate the positions of tumors. **B**, Tumor growth rates from mice injected with DEST#1 and DKK1#1. Diamond symbols indicate the tumor volume of mice injected with DEST#1; Box symbols indicate the tumor volume of mice injected with DKK1#1.
doi:10.1371/journal.pone.0004634.g007

Although SK-ES1-DKK2#2 xenografts were significantly larger than control SK-ES1-DEST xenografts, the clone SK-ES1-DKK2#1 presented no significant difference from SK-ES1-DEST clones (data not shown).

Discussion

In this study, we found that the expression of DKK2 was enhanced but that of DKK1 was suppressed in EFT cells. The suppression of DKK1 expression has been observed in several tumors [16,48,49,50], and although elevated level of the DKK family occur in a number of tumor cells, most reports to date have been concerned with DKK1 and DKK3 [15]. In the case of DKK2, its suppression in tumors such as malignant melanoma [17] and gastrointestinal tumors [51] has been reported, but the elevated levels in cancer have not. Hence, the expression profile of the DKK family observed here is suggested to be specific to EFT.

We also demonstrated that the expression of DKK2 is regulated by the direct interaction of the chimeric protein EWS/ETS with EBS located in the promoter region of the gene. In contrast, although we also investigated the effect of EWS/ETS on DKK1 transcription, EWS/ETS exhibited no significant effect on DKK1 promoter activity as assessed by the reporter assay. However, the induction of EWS/ETS expression in human MPCs resulted in not only an increase in DKK2 gene expression but also a considerable decrease in DKK1 gene expression. Moreover, introduction of the DKK2 gene induced a reduction in DKK1 gene expression and vice versa in SK-ES1 cell. Taken together, our results indicate that EWS/ETS expression in EFT cells directly induces the up-regulation of DKK2 gene expression that consequently leads to a suppression of DKK1 expression, although the further analysis is required for understanding the underlying mechanism of EWS/ETS-mediated modulation of DKK family expression.

Although DKK1 is known as a Wnt antagonist, the function of DKK2 is still controversial. Some studies indicated that DKK2 also acts as an antagonist of Wnt signaling, whereas others showed that DKK2 behaves rather agonistic to Wnt signaling. In some tumor types, Wnt antagonists including DKK1 act as tumor suppressors [19,20,24,52,53]. As we demonstrated in this study, ectopic expression of DKK1 in EFT cells resulted in the inhibition of tumor growth in SCID mice, whereas DKK2 expression did not and even possibly accelerated tumor growth *in vivo*, demonstrating that DKK2 does not act as a counterpart of DKK1. Therefore, our findings support reports that presented DKK2 has a distinct function from DKK1. As we described above, the up-regulation of DKK2 consequently leads to a suppression of DKK1 and thus possibly contributes to EFT phenotype indirectly by interfering with the suppressive function of DKK1 on tumor growth. To further investigate the role of DKK2 in EFT formation, we have tested the effect of temporal DKK2 knockdown by transient transfection with DKK2 siRNA, whereas no significant influence on cell growth and cell death was observed as assessed by MTT assay and Annexin V assay, respectively (data not shown). The further experiments to elucidate the direct effect of DKK2 on EFT phenotype are now underway.

Interestingly, it was recently suggested that DKK1 also functions independently of the canonical Wnt/β–catenin signaling pathway. For example, several studies have indicated that DKK1-mediated tumor suppression is independent of canonical Wnt/β–catenin signaling [20]. It was also reported that Wnt3A-mediated activation of the canonical Wnt/β–catenin signaling pathway induces neuritic outgrowth in EFT cells [54], and DKK1 mimics Wnt activity and induces neuritogenesis in EFT cells. Therefore, it is possible that DKK2 also has a function independent of Wnt signaling that is distinct from that of DKK1.

As described above, DKK1 has a significant function in hMPCs and could stimulate cell proliferation while maintaining the undifferentiated phenotype [55]. Therefore, adequate DKK expression is essential for the maintenance of the MPC phenotype. Although the origins of EFT are still unclear, hMPCs are thought to be a candidate [56,57] and we previously showed that inducible EWS/ETS expression in human MPCs confers EFT-like phenotypes [35]. Since, as we found in this study, EWS/ETS expression induces the down-regulation of DKK1 expression and up-regulation of DKK2 in UET-13 cells, an expression profile of the DKK family typical of EFT cells, it is reasonable to speculate that EWS/ETS-mediated change in the DKK family expression profile in hMPCs is involved in the development of EFT. Consistent with this, interestingly, a recent study revealed that the expression of DKK1 is up-regulated in EWS/FLI1-silenced EFT cells [58], in which feature of the mesenchymal progenitor including the capacity to differentiation into the osteogenic and adipogenic lineages are conferred. Considering the significance of DKK1 expression in hMPCs, EWS/ETS-mediated DKK1 suppression could impair the characteristics of hMPCs and contribute to their transformation into EFT.

Acknowledgments

We are grateful to T. Motoyama for the NRS-1 cell line. We respectfully thank S. Yamauchi for her secretarial work.

Author Contributions

Conceived and designed the experiments: YM HO NK. Performed the experiments: YM MI. Analyzed the data: YM. Contributed reagents/materials/analysis tools: YM MT YUK JF JiH AU. Wrote the paper: YM HO NK.

References

1. Mohinta S, Wu H, Chaurasia P, Watabe K (2007) Wnt pathway and breast cancer. Front Biosci 12: 4020–4033.
2. Reguart N, He B, Taron M, You L, Jablons DM, et al. (2005) The role of Wnt signaling in cancer and stem cells. Future Oncol 1: 787–797.
3. Segditsas S, Tomlinson I (2006) Colorectal cancer and genetic alterations in the Wnt pathway. Oncogene 25: 7531–7537.
4. Polakis P (2000) Wnt signaling and cancer. Genes Dev 14: 1837–1851.
5. Satoh S, Daigo Y, Furukawa Y, Kato T, Miwa N, et al. (2000) AXIN1 mutations in hepatocellular carcinomas, and growth suppression in cancer cells by virus-mediated transfer of AXIN1. Nat Genet 24: 245–250.
6. Kawano Y, Kypta R (2003) Secreted antagonists of the Wnt signalling pathway. J Cell Sci 116: 2627–2634.
7. Zorn AM (2001) Wnt signalling: antagonistic Dickkopfs. Curr Biol 11: R592–595.

8. Brott BK, Sokol SY (2002) Regulation of Wnt/LRP signaling by distinct domains of Dickkopf proteins. Mol Cell Biol 22: 6100–6110.
9. Mao B, Wu W, Li Y, Hoppe D, Stannek P, et al. (2001) LDL-receptor-related protein 6 is a receptor for Dickkopf proteins. Nature 411: 321–325.
10. Mukhopadhyay M, Shtrom S, Rodriguez-Esteban C, Chen L, Tsukui T, et al. (2001) Dickkopf1 is required for embryonic head induction and limb morphogenesis in the mouse. Dev Cell 1: 423–434.
11. Grotewold L, Theil T, Ruther U (1999) Expression pattern of Dkk-1 during mouse limb development. Mech Dev 89: 151–153.
12. Adamska M, MacDonald BT, Sarmast ZH, Oliver ER, Meisler MH (2004) En1 and Wnt7a interact with Dkk1 during limb development in the mouse. Dev Biol 272: 134–144.
13. Morvan F, Boulukos K, Clement-Lacroix P, Roman Roman S, Suc-Royer I, et al. (2006) Deletion of a single allele of the Dkk1 gene leads to an increase in bone formation and bone mass. J Bone Miner Res 21: 934–945.
14. Li J, Sarosi I, Cattley RC, Pretorius J, Asuncion F, et al. (2006) Dkk1-mediated inhibition of Wnt signaling in bone results in osteopenia. Bone 39: 754–766.
15. Niehrs C (2006) Function and biological roles of the Dickkopf family of Wnt modulators. Oncogene 25: 7469–7481.
16. Aguilera O, Fraga MF, Ballestar E, Paz MF, Herranz M, et al. (2006) Epigenetic inactivation of the Wnt antagonist DICKKOPF-1 (DKK-1) gene in human colorectal cancer. Oncogene 25: 4116–4121.
17. Kuphal S, Lodermeyer S, Bataille F, Schuierer M, Hoang BH, et al. (2006) Expression of Dickkopf genes is strongly reduced in malignant melanoma. Oncogene 25: 5027–5036.
18. Mikheev AM, Mikheeva SA, Rostomily R, Zarbl H (2007) Dickkopf-1 activates cell death in MDA-MB435 melanoma cells. Biochem Biophys Res Commun 352: 675–680.
19. Mikheev AM, Mikheeva SA, Maxwell JP, Rivo JV, Rostomily R, et al. (2007) Dickkopf-1 mediated tumor suppression in human breast carcinoma cells. Breast Cancer Res Treat.
20. Mikheev AM, Mikheeva SA, Liu B, Cohen P, Zarbl H (2004) A functional genomics approach for the identification of putative tumor suppressor genes: Dickkopf-1 as suppressor of HeLa cell transformation. Carcinogenesis 25: 47–59.
21. Tian E, Zhan F, Walker R, Rasmussen E, Ma Y, et al. (2003) The role of the Wnt-signaling antagonist DKK1 in the development of osteolytic lesions in multiple myeloma. N Engl J Med 349: 2483–2494.
22. Wirths O, Waha A, Weggen S, Schirmacher P, Kuhne T, et al. (2003) Overexpression of human Dickkopf-1, an antagonist of wingless/WNT signaling, in human hepatoblastomas and Wilms' tumors. Lab Invest 83: 429–434.
23. Edamura K, Nasu Y, Takaishi M, Kobayashi T, Abarzua F, et al. (2007) Adenovirus-mediated REIC/Dkk-3 gene transfer inhibits tumor growth and metastasis in an orthotopic prostate cancer model. Cancer Gene Ther 14: 765–772.
24. Hsieh SY, Hsieh PS, Chiu CT, Chen WY (2004) Dickkopf-3/REIC functions as a suppressor gene of tumor growth. Oncogene 23: 9183–9189.
25. Hoang BH, Kubo T, Healey JH, Yang R, Nathan SS, et al. (2004) Dickkopf 3 inhibits invasion and motility of Saos-2 osteosarcoma cells by modulating the Wnt-beta-catenin pathway. Cancer Res 64: 2734–2739.
26. Tsuji T, Miyazaki M, Sakaguchi M, Inoue Y, Namba M (2000) A REIC gene shows down-regulation in human immortalized cells and human tumor-derived cell lines. Biochem Biophys Res Commun 268: 20–24.
27. Lodygin D, Epanchintsev A, Menssen A, Diebold J, Hermeking H (2005) Functional epigenomics identifies genes frequently silenced in prostate cancer. Cancer Res 65: 4218–4227.
28. Khoury JD (2005) Ewing sarcoma family of tumors. Adv Anat Pathol 12: 212–220.
29. Fuchs B, Inwards CY, Janknecht R (2004) Vascular endothelial growth factor expression is up-regulated by EWS-ETS oncoproteins and Sp1 and may represent an independent predictor of survival in Ewing's sarcoma. Clin Cancer Res 10: 1344–1353.
30. Li X, Tanaka K, Nakatani F, Matsunobu T, Sakimura R, et al. (2005) Transactivation of cyclin E gene by EWS-Fli1 and antitumor effects of cyclin dependent kinase inhibitor on Ewing's family tumor cells. Int J Cancer 116: 385–394.
31. Takahashi A, Higashino F, Aoyagi M, Yoshida K, Itoh M, et al. (2003) EWS/ETS fusions activate telomerase in Ewing's tumors. Cancer Res 63: 8338–8344.
32. Nakatani F, Tanaka K, Sakimura R, Matsumoto Y, Matsunobu T, et al. (2003) Identification of p21WAF1/CIP1 as a direct target of EWS-Fli1 oncogenic fusion protein. J Biol Chem 278: 15105–15115.
33. Hahm KB, Cho K, Lee C, Im YH, Chang J, et al. (1999) Repression of the gene encoding the TGF-beta type II receptor is a major target of the EWS-FLI1 oncoprotein. Nat Genet 23: 222–227.
34. Im YH, Kim HT, Lee C, Poulin D, Welford S, et al. (2000) EWS-FLI1, EWS-ERG, and EWS-ETV1 oncoproteins of Ewing tumor family all suppress transcription of transforming growth factor beta type II receptor gene. Cancer Res 60: 1536–1540.
35. Miyagawa Y, Okita H, Nakaijima H, Horiuchi Y, Sato B, et al. (2008) Inducible expression of chimeric EWS/ETS proteins confers Ewing's family tumor-like phenotypes to human mesenchymal progenitor cells. Mol Cell Biol.
36. Yamashita J, Miyagawa Y, Sugahara R, Mon H, Mitsunobu H, et al. (2007) Molecular Cloning of Silkworm Cdc37 and its Interaction with Hsp90 Chaperone. J Insect Biotech Seric 76: 137–143.
37. Hara S, Ishii E, Tanaka S, Yokoyama J, Katsumata K, et al. (1989) A monoclonal antibody specifically reactive with Ewing's sarcoma. Br J Cancer 60: 875–879.
38. Fujii Y, Nakagawa Y, Hongo T, Igarashi Y, Naito Y, et al. (1989) [Cell line of small round cell tumor originating in the chest wall: W-ES]. Hum Cell 2: 190–191.
39. Mori T, Kiyono T, Imabayashi H, Takeda Y, Tsuchiya K, et al. (2005) Combination of hTERT and bmi-1, E6, or E7 induces prolongation of the life span of bone marrow stromal cells from an elderly donor without affecting their neurogenic potential. Mol Cell Biol 25: 5183–5195.
40. Gilbert F, Balaban G, Moorhead P, Bianchi D, Schlesinger H (1982) Abnormalities of chromosome 1p in human neuroblastoma tumors and cell lines. Cancer Genet Cytogenet 7: 33–42.
41. Nishi Y, Akiyama K, Korf BR (1992) Characterization of N-myc amplification in a human neuroblastoma cell line by clones isolated following the phenol emulsion reassociation technique and by hexagonal field gel electrophoresis. Mamm Genome 2: 11–20.
42. Hata J, Fujita H, Ikeda E, Matsubayashi Y, Kokai Y, et al. (1989) [Differentiation of human germ cell tumor cells]. Hum Cell 2: 382–387.
43. Miyagawa Y, Lee JM, Maeda T, Koga K, Kawaguchi Y, et al. (2005) Differential expression of a Bombyx mori AHA1 homologue during spermatogenesis. Insect Mol Biol 14: 245–253.
44. Kiyokawa N, Lee EK, Karunagaran D, Lin SY, Hung MC (1997) Mitosis-specific negative regulation of epidermal growth factor receptor, triggered by a decrease in ligand binding and dimerization, can be overcome by overexpression of receptor. J Biol Chem 272: 18656–18665.
45. Arvand A, Denny CT (2001) Biology of EWS/ETS fusions in Ewing's family tumors. Oncogene 20: 5747–5754.
46. Gregory CA, Perry AS, Reyes E, Conley A, Gunn WG, et al. (2005) Dkk-1-derived synthetic peptides and lithium chloride for the control and recovery of adult stem cells from bone marrow. J Biol Chem 280: 2309–2323.
47. Gregory CA, Singh H, Perry AS, Prockop DJ (2003) The Wnt signaling inhibitor dickkopf-1 is required for reentry into the cell cycle of human adult stem cells from bone marrow. J Biol Chem 278: 28067–28078.
48. Suzuki R, Onizuka M, Kojima M, Shimada M, Fukagawa S, et al. (2007) Preferential hypermethylation of the Dickkopf-1 promoter in core-binding factor leukaemia. Br J Haematol 138: 624–631.
49. Suzuki H, Toyota M, Caraway H, Gabrielson E, Ohmura T, et al. (2008) Frequent epigenetic inactivation of Wnt antagonist genes in breast cancer. Br J Cancer 98: 1147–1156.
50. Lee J, Yoon YS, Chung JH (2008) Epigenetic silencing of the WNT antagonist DICKKOPF-1 in cervical cancer cell lines. Gynecol Oncol 109: 270–274.
51. Sato H, Suzuki H, Toyota M, Nojima M, Maruyama R, et al. (2007) Frequent epigenetic inactivation of DICKKOPF family genes in human gastrointestinal tumors. Carcinogenesis 28: 2459–2466.
52. Roth W, Wild-Bode C, Platten M, Grimmel C, Melkonyan HS, et al. (2000) Secreted Frizzled-related proteins inhibit motility and promote growth of human malignant glioma cells. Oncogene 19: 4210–4220.
53. Joesting MS, Perrin S, Elenbaas B, Fawell SE, Rubin JS, et al. (2005) Identification of SFRP1 as a candidate mediator of stromal-to-epithelial signaling in prostate cancer. Cancer Res 65: 10423–10430.
54. Endo Y, Beauchamp E, Woods D, Taylor WG, Toretsky JA, et al. (2008) Wnt-3a and Dickkopf-1 stimulate neurite outgrowth in Ewing tumor cells via a Frizzled3- and c-Jun N-terminal kinase-dependent mechanism. Mol Cell Biol 28: 2368–2379.
55. Horwitz EM (2004) Dkk-1-mediated expansion of adult stem cells. Trends Biotechnol 22: 386–388.
56. Riggi N, Cironi L, Provero P, Suva ML, Kaloulis K, et al. (2005) Development of Ewing's sarcoma from primary bone marrow-derived mesenchymal progenitor cells. Cancer Res 65: 11459–11468.
57. Castillero-Trejo Y, Eliazer S, Xiang L, Richardson JA, Ilaria RL Jr. (2005) Expression of the EWS/FLI-1 oncogene in murine primary bone-derived cells Results in EWS/FLI-1-dependent, ewing sarcoma-like tumors. Cancer Res 65: 8698–8705.
58. Tirode F, Laud-Duval K, Prieur A, Delorme B, Charbord P, et al. (2007) Mesenchymal stem cell features of Ewing tumors. Cancer Cell 11: 421–429.

Leukemia Research 33 (2009) 908–912

Contents lists available at ScienceDirect

Leukemia Research

journal homepage: www.elsevier.com/locate/leukres

The expression of granulysin in systemic anaplastic large cell lymphoma in childhood

Noriko Kitamura[a,b], Yohko U. Katagiri[a], Mitsuko Itagaki[a], Yoshitaka Miyagawa[a], Keiko Onda[a], Hajime Okita[a], Akio Mori[b], Junichiro Fujimoto[a], Nobutaka Kiyokawa[a,*]

[a] Department of Developmental Biology, National Research Institute for Child Health and Development, 2-10-1 Okura, Setagaya-ku, Tokyo 157-8535, Japan
[b] Clinical Research Center for Allergy and Rheumatology, National Sagamihara Hospital, Sagamihara, Kanagawa 228-8522, Japan

ARTICLE INFO

Article history:
Received 9 May 2008
Received in revised form
29 December 2008
Accepted 26 January 2009
Available online 24 February 2009

Keywords:
Granulysin
Childhood lymphomas
Systemic anaplastic large cell lymphoma
T cells
NK cells
CD96
Cell origin

ABSTRACT

The expression of granulysin, a cytolytic protein produced by activated T and NK cells, has been revealed to be correlated with the prognosis of some adult cancer patients. By examination on various childhood lymphoma tissues, we found that granulysin level was especially high in systemic anaplastic large cell lymphoma (ALCL) cases, whereas no close correlation with the expression of CD96, a marker for activated T and NK cells, was observed. We further demonstrated that both ALCL cells in biopsy specimens and cell lines established from ALCL express granulysin, indicating some correlation of granulysin with biological features of ALCL.

1. Introduction

Granulysin is a cytolytic protein colocalized with other cytotoxic effectors in the granules of human activated T and NK cells [1,2]. Granulysin causes defects in negatively charged cholesterol-free membranes, a membrane composition typically found in bacteria, leading to both an elevation in the intracellular Ca^{2+} concentration and an increase in ceramide. As a consequent, mitochondria are damaged, causing the release of cytochrome c and apoptosis is induced [3–6]. In contrast, granulysin is able to bind to lipid rafts in eukaryotic cell membranes, where it is taken up by the endocytotic pathway, leaving the cell intact [6]. To date, two actions of granulysin have been described [2,7]. First, granulysin has an antibacterial effect and its antimicrobial activity against *Mycobacterium tuberculosis* as well as *Cryptococcus neoformans* has been shown to be dependent on the expression level of granulysin in cytotoxic T cells [8–12]. Second, granulysin reveals antitumoral activity. Many studies suggest that granulysin is an effective antitumor protein [2,7]. In experiments using an animal model, human granulysin promoted survival in transgenic mice with tumors [13]. Granulysin protein levels in NK cells were correlated with the prognosis or progression of disease in adult cancer patients [14,15]. However, the correlation between granulysin and clinicopathological features of childhood cancers, including lymphoma, is yet to be clarified.

There are four major types of childhood non-Hodgkin lymphoma; lymphoblastic lymphoma (LBL), Burkitt lymphoma, diffuse large B cell lymphoma and systemic anaplastic large cell lymphoma (ALCL), each with its own prognosis. ALCL is characterized by specific large lymphoma cells expressing CD30 frequently with chromosomal translocations that generate chimeric gene NPM-ALK in which the anaplastic lymphoma kinase (ALK) gene is involved [16–18]. ALCL has a T cell- or null cell-like phenotype and in some cases perforin and other cytotoxic effectors are expressed, suggesting ALCL originates from cytotoxic T or NK cells [19,20]. ALCL in childhood generally has a relatively good prognosis, however, clinicopathologic differences exist and some patients do poorly. Biological variation including the presence of NPM-ALK-positive and -negative cases indicates ALCL to be a heterogeneous disease type [17].

In an attempt to clarify the expressional state of granulysin in childhood lymphoma, we examined the mRNA expression of granulysin in tissues obtained from various cases of childhood lymphoma including ALCL. In this paper, we present a difference in granulysin expression among the types of childhood lymphomas.

* Corresponding author. Tel.: +81 3 3416 0181; fax: +81 3 3417 2864.
E-mail address: nkiyokawa@nch.go.jp (N. Kiyokawa).

0145-2126/$ – see front matter © 2009 Elsevier Ltd. All rights reserved.
doi:10.1016/j.leukres.2009.01.032

Notably, ALCLs had high levels of granulysin. The biological effect of granulysin in ALCL is discussed.

2. Materials and methods

2.1. Materials

Biopsy specimens from pediatric patients, including ten patients with ALCL, four with precursor B (B)-LBL, six with Burkitt lymphoma, five with diffuse large B cell lymphoma, five with Hodgkin's lymphoma and eight with precursor T (T)-LBL, were selected from files between 1985 and 2001 at our laboratory. In each case, the initial diagnosis was based on morphological observations and the immunophenotypic characteristics. The specimens are now kept under conditions of anonymity and all of the experiments included in this study followed the tenets of the Declaration of Helsinki and were performed with the approval of the local ethics committee.

The human ALCL cell lines Karpas-299 (a gift from Dr. K. Kikuchi of Sapporo Medical College, Sapporo, Japan) and SUDHL-1, the human Burkitt lymphoma cell line BALM-24 (gifts from Cell Biology Institute, Research Center, Hayashibara Biochemical Laboratories, Inc., Okayama, Japan), and the human megakaryoblastic cell lines CMK (a gift from Dr. T. Sato of Chiba University, School of Medicine, Chiba, Japan), Dami (American Type Culture Collection, Manassas, VA) and Meg-01 (Institute of Fermentation, Osaka, Japan) were used. Cells were maintained in RPMI1640 medium supplemented with 10% fetal calf serum at 37 °C in a humidified 5% CO_2 atmosphere. Mononuclear cells obtained from the peripheral blood of healthy volunteers by Ficoll-Paque centrifugation were cultured for 24 h in the presence of 5 nM of 12-myristate 13 acetate (PMA, Sigma–Aldrich Fine Chemical Co., St. Louis, MO) and 1 μM of ionomycin (Sigma) and collected for the extraction of total RNA.

2.2. RT-PCR and real-time PCR

Each tissue was embedded in optimal cutting temperature (O.C.T.) compound under rapid freezing conditions. The frozen tissues were sliced up 5-μm thick by cryostat, homogenized in Isogen (Nippon gene, Toyama, Japan). Total RNA was extracted according to the manufacturer's protocol. Using 1 μg of total RNA, cDNA was synthesized by transcriptase (Amersham Biosciences, Buckinghamshire, UK) and expression of granulysin mRNA was determined by quantitative real-time PCR using Taqman MGB probe with ABI 7900 systems (ABI, Foster City, CA).

2.3. Flow cytometry and immunohistochemical staining

To detect the cytoplasmic expression of granulysin, cells sequentially fixed with 4% paraformaldehyde followed by 70% ethanol were stained with fluorescein isothiocyanate (FITC)-labeled mouse anti-granulysin monoclonal antibody (RC8, Medical & Biological Laboratories, Co., Ltd., MBL, Nagoya, Japan) and examined by flow cytometry (EPICS-XL, Beckman Coulter, Inc., Fullerton, CA).

For immunohistochemical staining, the formalin-fixed, paraffin-embedded tissue specimens were deparafinized, treated using the heat-induced epitope retrieval method in 10 mM of citrate buffer, pH 6.0, stained with a combination of Alexa Fluor™546 (Invitrogen, Co., Carsbad, CA)-labeled rabbit anti-granulysin polyclonal antibody (Santa Cruz Biotechnology, Inc., Santa Crus, CA) and Alexa Fluor™488-labeled anti-ALK monoclonal antibody (ALK-C, Beckman) and examined by immunofluorescence microscopy (Olympus, Co., Tokyo, Japan). Photographs were taken with a CCD Camera (Cascade, Roper Scientific, Inc., Tucson, AZ).

The peripheral blood-derived mononuclear cells cultured for 5 days as described above were cytocentrifuged on slide glasses by using Cytospin II (Shandon, Inc., Pittsburgh, PA) and fixed with 4% paraformaldehyde. Cytochemical staining was performed by using either mouse monoclonal anti-granulysin antibody (RC8) or rabbit anti-granulysin polyclonal antibody as described above.

2.4. Statistical analysis

The statistical analysis was performed with a nonparametric Mann–Whitney test and correlations were determined using nonparametric statistics. A p-value less than 0.05 was considered to be statistically significant.

3. Results

First, to verify any differences in the level of granulysin expression between the types of lymphoma in childhood, we performed a quantitative real-time PCR analysis with total RNA extracted from the tumor tissues obtained from pediatric patients with ALCL, B-LBL, Burkitt, diffuse large B cell lymphoma, Hodgkin, and T-LBL. As shown in Fig. 1, the pattern of granulysin expression differed in each type of lymphoma. When compared with the value normalized to be expression of GAPDH, the level of granulysin was particularly high in ALCL (mean intensity normalized with GAPDH = 1.066),

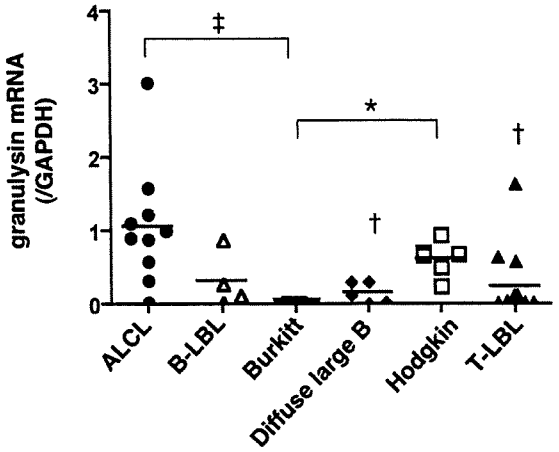

Fig. 1. Expression of granulysin mRNA in childhood lymphoma cases. The granulysin mRNA levels in extirpated tissues were determined with real-time quantitative PCR. Each value is normalized to GAPDH expression in the sample. ALCL, systemic anaplastic large cell lymphoma; B-LBL, precursor B lymphoblastic lymphoma; T-LBL, precursor T lymphoblastic lymphoma. The Burkitt cases ($^{\ddagger}p < 0.001$), diffuse large B cases ($^{\dagger}p < 0.01$) and T-LBL cases ($^{\dagger}p < 0.01$) exhibited significantly low levels of granulysin mRNA in comparison with the ALCL cases. The Burkitt cases ($^{*}p < 0.01$) showed significantly low levels in comparison with the Hodgkin cases.

while the level in Burkitt lymphoma was very low (mean intensity = 0.012) and that in Hodgkin lymphoma was moderate (mean intensity = 0.625). Some significant differences between the types were observed: ALCL vs. Burkitt, $p < 0.001$; ALCL vs. Diffuse large B- or T-LBL, $p < 0.01$; Burkitt vs. Hodgkin, $p < 0.01$.

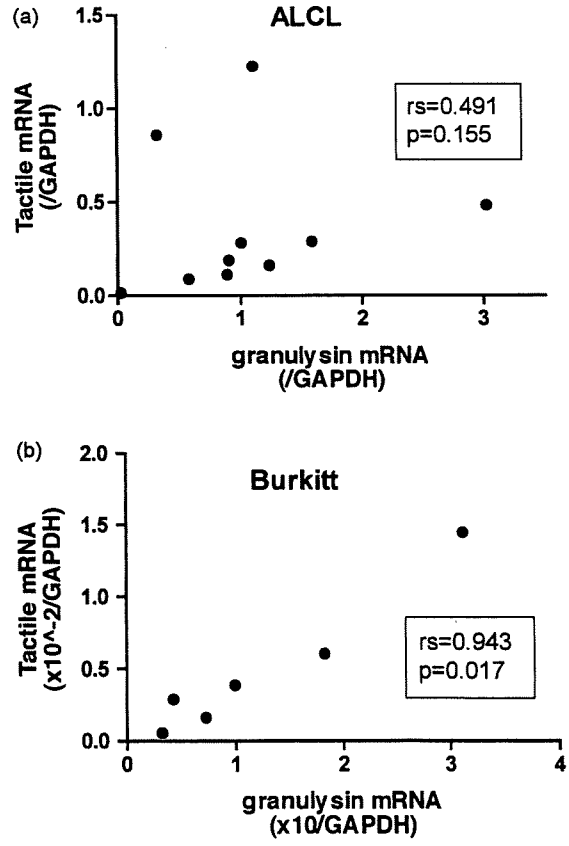

Fig. 2. Analysis of the correlation between granulysin and CD96 mRNA expression in childhood lymphoma cases. The mRNA expression of CD96 in the ALCL cases (a) and Burkitt cases (b) was examined and the correlation between granulysin and CD96 mRNA expression was evaluated.

The difference in granulysin expression was possibly influenced by the number of activated cytotoxic T and/or NK cells that had infiltrated into the tissues. Therefore, we examined the expression of a marker gene for cytotoxic T and NK cells and compared it with that of granulysin. CD96, also called T cell-activated increased late expression (TACTILE), is involved in the adhesion of activated T and NK cells late in an immune response and one of the several markers of activated T or NK cells [21]. In fact, its expression has been demonstrated to be well correlated with that of granulysin in some cancer patients [1,21]. Thus, we selected CD96 to confirm from where the granulysin mRNA was derived. Although the expression of CD96 mRNA was observed to be closely correlated with the expression of granulysin in Burkitt cases ($rs = 0.943$, $p < 0.05$) (Fig. 2b), no significant correlation between the expressions of these two molecules in ALCL cases ($rs = 0.491$) was obtained (Fig. 2a).

In some cases, ALCL cells express cytotoxic molecules such as perforin and granzyme B and thus have been suggested to be directed from cytotoxic T or NK cells. Considering the above results, we hypothesized that ALCL cells themselves express granulysin. Therefore, we used the ALCL-derived cell lines Karpas-299 and SUDHL-1 and determined the expression of granulysin in these cells. As shown in Fig. 3, granulysin mRNA was expressed in these cell lines as well as activated peripheral blood mononuclear cells and the megakaryoblastic cell line CMK. However, the mRNA was not detected in the megakaryoblastic cell lines Daudi and Meg-01 (Fig. 3a) and Burkitt lymphoma cell lines including BALM-24 (data

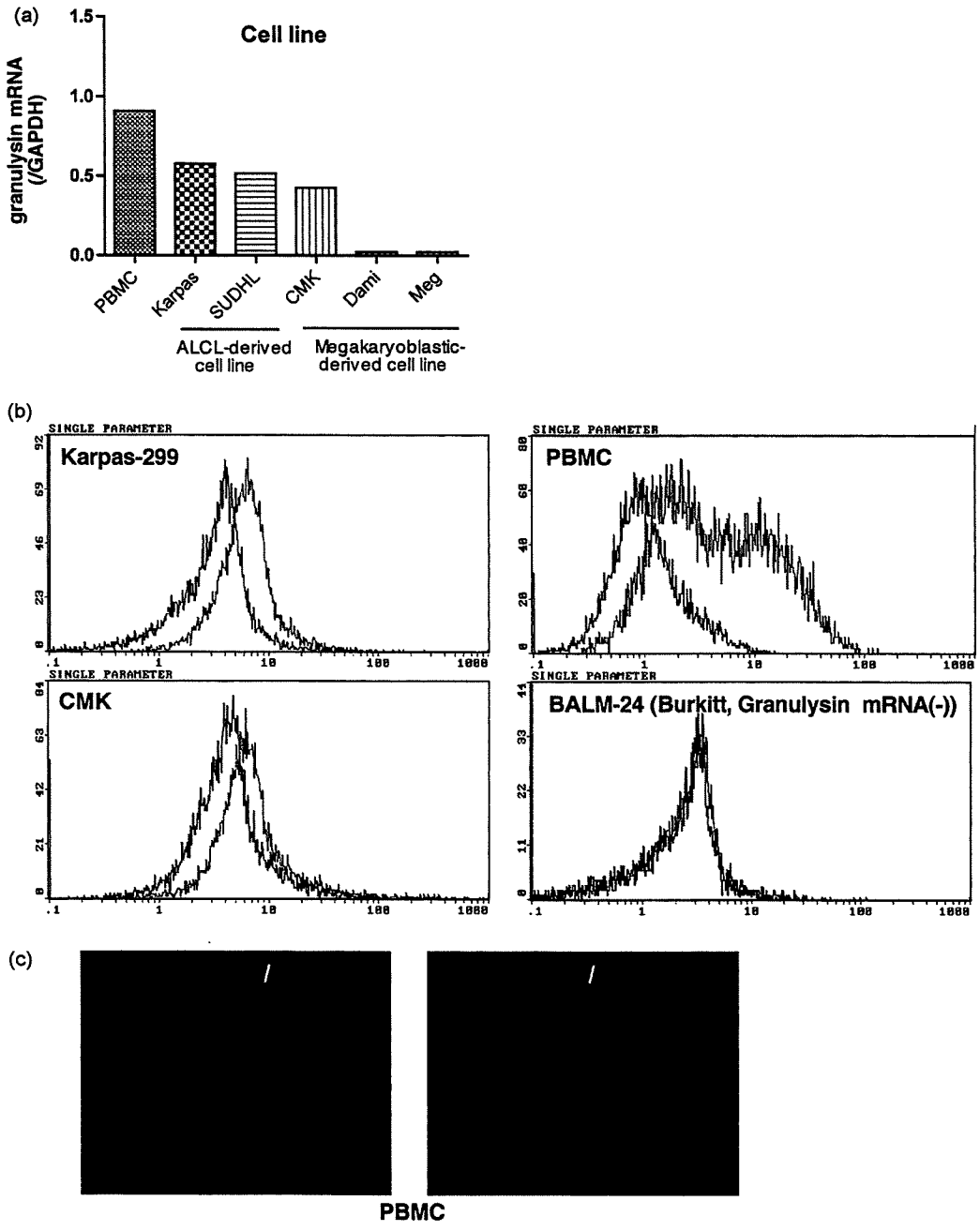

Fig. 3. Expression of granulysin in ALCL cell lines. (a) The levels of granulysin mRNA in ALCL-derived cell lines (Karpas-299 and SUDHL-1) and megakaryoblastic-derived cell lines (CMK, Dami and Meg-01) were determined. As a positive control, activated peripheral blood mononuclear cells (PBMC) were also examined. (b) Cytoplasmic expression of granulysin in Karpas-299, CMK, Burkitt lymphoma BALM-24 and PBMC was examined by using flow cytometry. (c) Cytoplasmic localization of granulysin in PBMC was also confirmed by cytochemical staining. As a negative control, the same sample specimen was also stained with control mouse IgG.

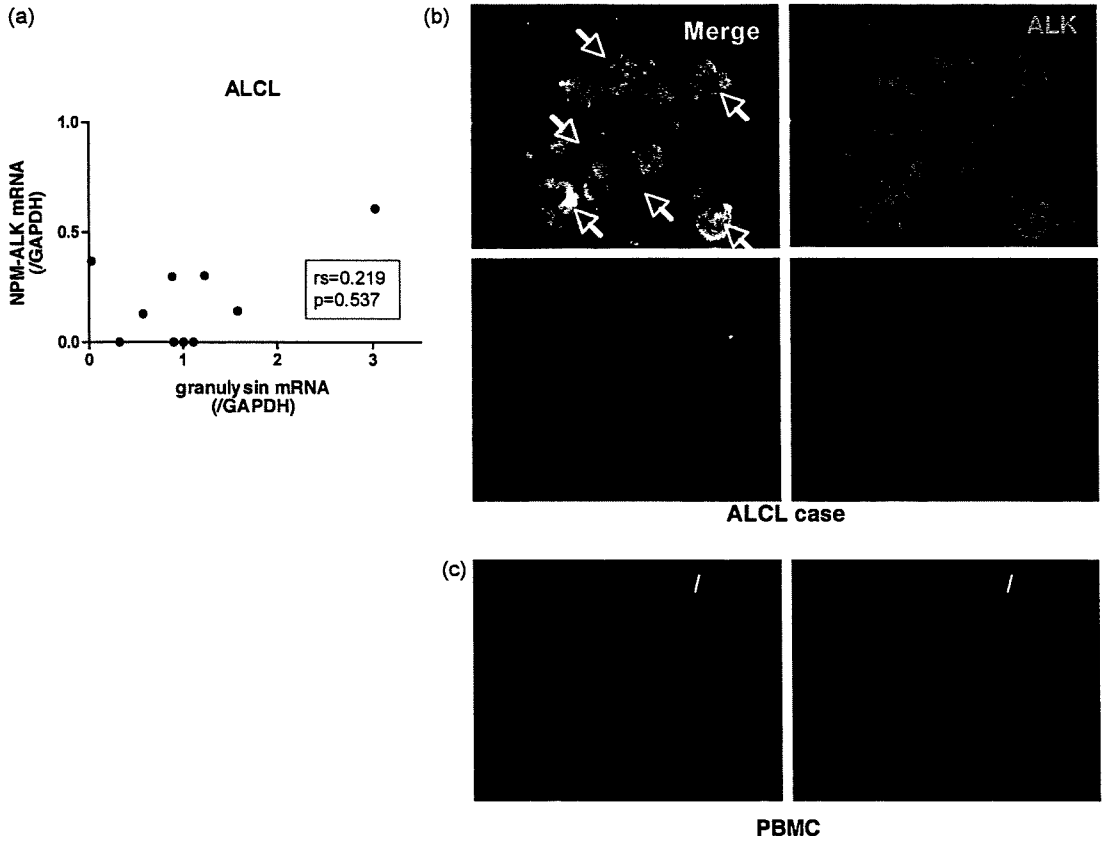

Fig. 4. Expression of granulysin in ALCL cases. (a) The mRNA expression of NPM-ALK in the ALCL cases was examined and the correlation between granulysin and NPM-ALK mRNA expression was evaluated. (b) The paraffin-embedded sections of ALCL cases were tested for dual color immunohistochemical staining using anti-granulysin antibody and anti-ALK antibody and examined by using immunofluorescence microscopy. A result representative of five ALCL cases is presented. (c) To confirm the specificity of anti-granulysin antibody, activated peripheral blood mononuclear cells were examined similarly. As a negative control, the same sample specimen was also stained with control rabbit IgG.

not shown). By employing flow cytometry, we further confirmed that granulysin protein is expressed in Karpas-299 and CMK cells but not in BALM-24 cells (Fig. 3b). We also confirmed the specificity of the granulysin staining using activated peripheral blood mononuclear cells (Fig. 3b and c).

NPM-ALK is a specific chimera gene for ALCL cells. To verify that granulysin is indeed expressed in ALCL cells in the tissue specimens, next we examined the expression of NPM-ALK in the ALCL cases and compared it with that of granulysin. As shown in Fig. 4a, NPM-ALK mRNA expression was observed in 60% of ALCL cases in this study, but the expression did not correlate with that of granulysin ($rs = 0.219$). We further examined the protein expression of ALK and granulysin in ALCL cases by employing dual color immunohistostaining in paraffin-embedded tissue. In granulysin-positive cases, granulysin protein was detected in ALK+ ALCL cells (Fig. 4b, yellow arrow). In addition, granulysin was also detected in ALK− small round cells (Fig. 4b, white arrow), most likely activated T or NK cells, in some cases. We also confirmed the specificity of the granulysin staining using activated peripheral blood mononuclear cells (Fig. 4c). Based on the above data, we concluded that granulysin can be expressed in both activated T or NK cells and ALCL cells themselves in ALCL cases.

It was reported that it some cases of ALCL, perforin, another cytotoxic molecule, is expressed. Thus, next we examined whether levels of perforin in ALCL patients were also increased because granulysin and perforin colocalized in activated T and NK cell granules. Though perforin mRNA expression was seen in 90% of cases, no correlation with granulysin was observed in ALCL ($rs = 0.382$) (Fig. 5).

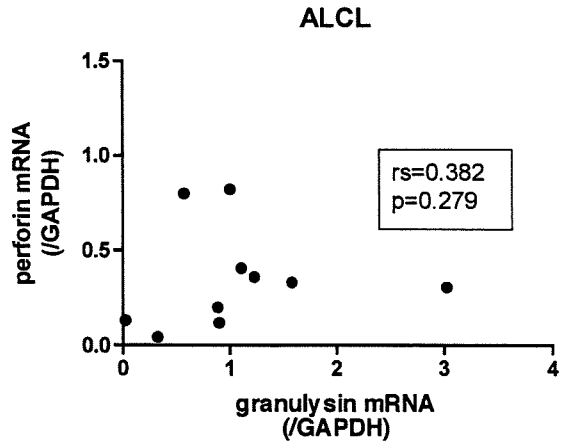

Fig. 5. Analysis of the correlation between granulysin and perforin mRNA expression in ALCL cases. The mRNA expression of perforin in the ALCL cases was examined and the correlation between granulysin and perforin mRNA expression was evaluated.

4. Discussion

The significance of activated T and NK cells, as well as the effect of granulysin produced by these cells, in childhood lymphoma tissues has yet to be clarified. In this study, we investigated the expression of granulysin in childhood cases of different lymphomas and found that the pattern of expression varied. As demonstrated in Fig. 1, level of granulysin was especially high in ALCL cases. Since the major

source of granulysin is generally thought to be activated T and NK cells [1,2], the expression in lymphomas might be dependent on the number of these cells that have infiltrated into tumor tissues. However, we observed that granulysin expression was not necessary correlated with CD96 expression in ALCL tissues (Fig. 2), suggesting that the granulysin expressed in ALCL tissues is not derived only from activated T or NK cells.

Since ALCLs often express cytotoxic effectors such as perforin and granzyme B, it has been postulated that they originate from cytotoxic lymphocytes [19,20]. Therefore, we hypothesized that the ALCL cells themselves express granulysin. Indeed, as we described above, the ALCL-derived cell lines Karpas-299 and SUDHL-1 expressed granulysin mRNA and protein (Fig. 3). Moreover, we detected granulysin protein in ALCL cells in clinical samples with immunohistochemical staining. As shown in Fig. 4b, the protein was detected both in ALK+ ALCL cells and in ALK− small round cells. Therefore, it is suggested that not only activated T and NK cells but also the ALCL cancers themselves express granulysin.

In activated T and NK cells, granulysin is colocalized with perforin in toxic granules, thus we also examined the mRNA expression of perforin in ALCL, but found that it was not correlated with the mRNA expression of granulysin. Therefore, it is suggested that the granulysin in ALCL cells is expressed independent of perforin. Since the expression of granzyme B was not correlated with that of perforin in ALCL cells either, the regulatory mechanism for the production of cytotoxic effectors in ALCL cells may be disorganized. Further investigation to elucidate the significance and molecular basis of granulysin expression in ALCL cells should provide information on the biological characteristics of ALCL, including a clue as to the cellular origin of this lymphoma.

Childhood ALCL has a relatively good prognosis and the relapse-free survival rate with first-line chemotherapy is 60–80% [18,22,23]. However, variation in clinicopathological features is recognized and in some cases the prognosis is poor. Since a way to predict the likely course of ALCL has yet to be established [17], searching for new markers that have a co-relation with prognosis is important. As we discussed above, it would be worth investigating the correlation between prognosis and the level of granulysin in ALCL cases. The question of how the expression of granulysin in the ALCL cells themselves affects the clinical course of ALCL is of particular interest.

In conclusion, we have investigated the expression of granulysin in childhood lymphomas and observed especially high levels in ALCL cases. Besides the activated T and NK cells, our findings indicated that the ALCL cells themselves expressed granulysin. Further elucidation of the biological significance of granulysin expression in ALCL should contribute to a better understanding of the biological features as well as underlying pathogenic mechanisms of this lymphoma.

Conflict of interest

None.

Acknowledgements

We thank S. Yamauchi for excellent secretarial work. This work was supported in part by a grant from JSPS. KAKENHI (No. 18790750) and Health and Labour Sciences Research Grants the 3rd term comprehensive 10-year-strategy for cancer control from the Ministry of Health, Labour and Welfare of Japan (No. H19-010).

Contributions. N. Kitamura and N. Kiyokawa contributed to the concept and design, interpreted and analyzed the data, provided drafting of the article, gave final approval, and obtained funding sources. K. Onda, Y.U. Katagiri, M. Itagaki, and Y. Miyagawa provided administrative support. H. Okita, A. Mori, and J. Fujimoto provided critical revisions and important intellectual content.

References

[1] Peña SV, Hanson DA, Carr BA, Goralski TJ, Krensky AM. Processing, subcellular localization, and function of 519 (granulysin), a human late T cell activation molecule with homology to small, lytic, granule proteins. J Immunol 1997;158:2680–8.
[2] Peña SV, Krensky AM. Granulysin, a new human cytolytic granule-associated protein with possible involvement in cell-mediated cytotoxicity. Semin Immunol 1997;9:117–25.
[3] Gamen S, Hanson DA, Kaspar A, Naval J, Krensky AM, Anel A. Granulysin-induced apoptosis. I. Involvement of at least two distinct pathways. J Immunol 1998;161:1758–64.
[4] Kaspar AA, Okada S, Kumar J, Poulain FR, Drouvalakis KA, Kelekar A, et al. A distinct pathway of cell-mediated apoptosis initiated by granulysin. J Immunol 2001;167:350–6.
[5] Okada S, Li Q, Whitin JC, Clayberger C, Krensky AM. Intracellular mediators of granulysin-induced cell death. J Immunol 2003;171:2556–62.
[6] Barman H, Walch M, Latinovic-Golic S, Dumrese C, Dolder M, Groscurth P, et al. Cholesterol in negatively charged lipid bilayers modulates the effect of the antimicrobial protein granulysin. J Membr Biol 2006;212:29–39.
[7] Wang Z, Choice E, Kaspar A, Hanson DA, Okada S, Lyu SC, et al. Bactericidal and tumoricidal activities of synthetic peptides derived from granulysin. J Immunol 2000;165:1486–90.
[8] Stenger S, Hanson DA, Teitelbaum R, Dewan P, Niazi KR, Froelich CJ, et al. An antimicrobial activity of cytolytic T cells mediated by granulysin. Science 1998;282:121–5.
[9] Ernst WA, Thoma-Uszynski S, Teitelbaum R, Ko C, Hanson DA, Clayberger C, et al. Granulysin, A T cell product. Kills bacteria by altering membrane permeability. J Immunol 2000;165:7102–8.
[10] Ma LL, Spurrell JC, Wang JF, Neely GG, Epelman S, Krensky AM, et al. CD8 T cell-mediated killing of *Cryptococcus neoformans* requires granulysin and is dependent on CD4 T cells and IL-15. J Immunol 2002;169:5787–95.
[11] Stegelmann F, Bastian M, Swoboda K, Bhat R, Kiessler V, Krensky AM, et al. Coordinate expression of CC chemokine ligand 5, granulysin, and perforin in CD8+ T cells provides a host defense mechanism against *Mycobacterium tuberculosis*. J Immunol 2005;175:7474–83.
[12] Sahiratmadja E, Alisjahbana B, Buccheri S, Di Liberto D, de Boer T, Adnan I, et al. Plasma granulysin levels and cellular interferon-gamma production correlate with curative host responses in tuberculosis, while plasma interferon-gamma levels correlate with tuberculosis disease activity in adults. Tuberculosis 2007;87:312–21.
[13] Huang LP, Lyu S, Clayberger C, Krensky AM. Granulysin-mediated tumor rejection in transgenic mice. J Immunol 2007;178:77–84.
[14] Kishi A, Takamori Y, Ogawa K, Takano S, Tomita S, Tanigawa M, et al. Differential expression of granulysin and perforin by NK cells in cancer patients and correlation of impaired granulysin expression with progression of cancer. Cancer Immunol Immunother 2002;50:604–14.
[15] Muris JJ, Meijer CJ, Cillessen SA, Vos W, Kummer JA, Bladergroen BA, et al. Prognostic significance of activated cytotoxic T-lymphocytes in primary nodal diffuse large B-cell lymphomas. Leukemia 2004;18:589–96.
[16] Stein H, Mason DY, Gerdes J, O'Connor N, Wainscoat J, Pallesen G, et al. The expression of the Hodgkin's disease-associated antigen Ki-1 in reactive and aneoplastic lymphoid tissue; evidence that Reed-Sternberg cells and histiocytic malignancies are derived from activated lymphoid cells. Blood 1985;66:848–58.
[17] Nakamura S, Shiota M, Nakagawa A, Yatabe Y, Kojima M, Motoori T, et al. Anaplastic large cell lymphoma: a distinct molecular pathologic entity: a reappraisal with special reference to p80 (NPM/ALK) expression. Am J Surg Pathol 1997;21:1420–32.
[18] Drexler HG, Gignac SM, von Wasielewski R, Werner M, Dirks WG. Pathology of *NPM-ALK* and variant fusion genes in anaplastic large cell lymphoma and other lymphomas. Leukemia 2000;14:1533–59.
[19] Foss H, Anagnostopoulos I, Araujo I, Assaf C, Demel G, Kummer JA, et al. Anaplastic large-cell lymphomas of T-cell and Null-cell phenotype express cytotoxic molecules. Blood 1996;88:4005–11.
[20] Krenacs L, Wellmann A, Sorbara L, Himmelmann AW, Bagdi E, Jaffe ES, et al. Cytotoxic cell antigen expression in anaplastic large cell lymphomas of T- and null cell type and Hodgkin's disease: evidence for distinct cellular origin. Blood 1997;89:980–9.
[21] Wang PL, O'Farrell S, Clayberger C, Krensky AM. Identification and molecular cloning of Tactile. A novel human T cell activation antigen that is a member of the Ig gene superfamily. J Immunol 1992;148:2600–8.
[22] Mori T, Kiyokawa N, Shimada H, Miyauchi J, Fujimoto J. Anaplastic large cell lymphoma in Japanese children: retrospective analysis of 34 patients diagnosed at the National Research Institute for Child Health and Development. Br J Haematol 2003;121:94–6.
[23] Mori T, Takimoto T, Katano N, Kikuchi A, Tabuchi K, Kobayashi R, et al. Recurrent childhood anaplastic large cell lymphoma: a retrospective analysis of registered cases in Japan. Br J Haematol 2006;132:594–7.

Immunology
The Journal of cells, molecules, systems and technologies

British Society for immunology

IMMUNOLOGY ORIGINAL ARTICLE

Ex vivo expanded cord blood CD4 T lymphocytes exhibit a distinct expression profile of cytokine-related genes from those of peripheral blood origin

Yoshitaka Miyagawa,[1] Nobutaka Kiyokawa,[1] Nakaba Ochiai,[2,3] Ken-Ichi Imadome,[4] Yasuomi Horiuchi,[1] Keiko Onda,[1] Misako Yajima,[4] Hiroyuki Nakamura,[4] Yohko U. Katagiri,[1] Hajime Okita,[1] Tomohiro Morio,[2,5] Norio Shimizu,[2,6] Junichiro Fujimoto[7] and Shigeyoshi Fujiwara,[4]

[1]*Department of Developmental Biology, National Research Institute for Child Health and Development, Setagaya-ku,* [2]*Center for Cell Therapy, Tokyo Medical and Dental University Medical Hospital, Bunkyo-ku, Tokyo,* [3]*Lymphotec Inc., Koto-ku, Tokyo,* [4]*Department of Infectious Diseases, National Research Institute for Child Health and Development, Setagaya-ku, Tokyo,* [5]*Department of Pediatrics and Developmental Biology, Graduate School of Medicine, Tokyo Medical and Dental University, Bunkyo-ku, Tokyo,* [6]*Department of Virology, Division of Medical Science, Medical Research Institute, Tokyo Medical and Dental University, Bunkyo-ku, Tokyo, and* [7]*Vice Director General, National Research Institute for Child Health and Development, Setagaya-ku, Tokyo, Japan*

Summary

With an increase in the importance of umbilical cord blood (CB) as an alternative source of haematopoietic progenitors for allogenic transplantation, donor lymphocyte infusion (DLI) with donor CB-derived activated $CD4^+$ T cells in the unrelated CB transplantation setting is expected to be of increased usefulness as a direct approach for improving post-transplant immune function. To clarify the characteristics of activated $CD4^+$ T cells derived from CB, we investigated their mRNA expression profiles and compared them with those of peripheral blood (PB)-derived activated $CD4^+$ T cells. Based on the results of a DNA microarray analysis and quantitative real-time reverse transcriptase–polymerase chain reaction (RT-PCR), a relatively high level of forkhead box protein 3 (Foxp3) gene expression and a relatively low level of interleukin (IL)-17 gene expression were revealed to be significant features of the gene expression profile of CB-derived activated $CD4^+$ T cells. Flow cytometric analysis further revealed protein expression of Foxp3 in a portion of CB-derived activated $CD4^+$ T cells. The low level of retinoic acid receptor-related orphan receptor γ isoform t (RORγt) gene expression in CB-derived activated $CD4^+$ T cells was speculated to be responsible for the low level of IL-17 gene expression. Our data indicate a difference in gene expression between $CD4^+$ T cells from CB and those from PB. The findings of Foxp3 expression, a characteristic of regulatory T cells, and a low level of IL-17 gene expression suggest that CB-derived $CD4^+$ T cells may be a more appropriate source for DLI.

Keywords: CD4; cord blood; donor lymphocyte infusion; forkhead box protein 3; interleukin 17; T cell

doi:10.1111/j.1365-2567.2009.03122.x
Received 1 September 2008; revised 30 March 2009; accepted 15 April 2009.
Correspondence: N. Kiyokawa, MD, PhD, Department of Developmental Biology, National Research Institute for Child Health and Development, 2-10-1, Okura, Setagaya-ku, Tokyo 157-8535, Japan.
Email: nkiyokawa@nch.go.jp
Senior author: Nobutaka Kiyokawa

Abbreviations: BIM, BCL2-like 11; CB, cord blood; CTLA-4, cytotoxic T-lymphocyte antigen-4; CDKN, cyclin-dependent kinase inhibitor; DLI, donor lymphocyte infusion; Foxp3, forkhead box protein 3; GAPDH, glyceraldehyde-3-phosphate dehydrogenase; GM-CSF, granulocyte–macrophage colony-stimulating factor; GVHD, graft-versus-host disease; GVL, graft-versus-leukaemia; HSCT, haematopoietic stem cell transplantation; ICOS, inducible T-cell co-stimulator; IFNG, interferon γ; IL, interleukin; PB, peripheral blood; RORγt, retinoic acid receptor-related orphan receptor γ isoform t; RT, reverse transcriptase; TCR, T-cell receptor; Th, T helper cell; Treg, regulatory T cell.

Introduction

Donor lymphocyte infusion (DLI) is a direct and useful approach for improving post-transplant immune function. DLI has been shown to exert a graft-versus-leukaemia (GVL) effect and has emerged as an effective strategy for the treatment of patients with leukaemia, especially chronic myelogenous leukaemia, who have relapsed after unrelated haematopoietic stem cell transplantation (HSCT).[1] In addition, DLI has been successfully used for some life-threatening viral infections, including Epstein–Barr virus and cytomegalovirus infections after HSCT.[2]

Although DLI frequently results in significant acute and/or chronic graft-versus-host disease (GVHD), several groups have demonstrated that depletion of CD8 T cells from DLIs efficiently reduces the incidence and severity of GVHD while maintaining GVL activity.[3,4] Therefore, selective CD4 DLI is expected to provide an effective and low-toxicity therapeutic strategy for improving post-transplant immune function. Actually, selective CD4 DLI based on a recently established method for *ex vivo* T-cell expansion using anti-CD3 monoclonal antibody and interleukin (IL)-2 is now becoming established as a routine therapeutic means of resolving post-transplant immunological problems in Japan.[5]

The importance of umbilical cord blood (CB) as an alternative source of haematopoietic progenitors for allogenic transplantation, mainly in patients lacking a human leucocyte antigen (HLA)-matched marrow donor, has increased in recent years. Because of the naïve nature of CB lymphocytes, the incidence and severity of GVHD are reduced in comparison with the allogenic transplant setting. In addition, CB is rich in primitive $CD16^-$ $CD56^+$ natural killer (NK) cells, which possess significant proliferative and cytotoxic capacities, and so have a substantial GVL effect.[6]

In contrast, a major disadvantage of CB transplantation is the low yield of stem cells, resulting in higher rates of engraftment failure and slower engraftment compared with bone marrow transplantation. In addition, it was generally thought to be difficult to perform DLI after CB transplantation using donor peripheral blood (PB), with the exception of transplantations from siblings. However, the above-described method for the *ex vivo* expansion of activated T cells can produce a sufficient amount of cells for therapy using the CB cell residues in an infused bag, which has solved this problem and made it possible to perform DLI with donor CB-derived activated $CD4^+$ T cells in the unrelated CB transplantation setting.[5] It has also been reported that CB-derived T cells can be expanded *ex vivo* while retaining the naïve and/or central memory phenotype and polyclonal T-cell receptor (TCR) diversity,[7] and thus potential utilization for adoptive cellular immunotherapy post-CB transplantation has been suggested.[8]

There are functional differences between CB and PB lymphocytes, although the details remain unclear. In an attempt to clarify the differences in characteristics between activated $CD4^+$ T cells derived from CB and those derived from PB, we investigated gene expression profiles. In this paper we present evidence that CB-derived $CD4^+$ T cells are distinct from PB-derived $CD4^+$ T cells in terms of gene expression.

Materials and methods

Cell culture and preparation

CB was distributed by the Tokyo Cord Blood Bank (Tokyo, Japan). The CB was originally collected and stored for stem cell transplantation. Stocks that were inappropriate for transplantation because they contained too few cells were distributed for research use with informed consent, with the permission of the ethics committee of the bank. In addition, all of the experiments in this study using distributed CB were performed with the approval of the local ethics committee. The mononuclear cells were isolated by Ficoll-Paque centrifugation and cultured in the presence of an anti-CD3 monoclonal antibody and interleukin (IL)-2 using TLY Culture Kit 25 (Lymphotec Inc., Tokyo, Japan) as described previously.[5] Although several different methods for T-cell stimulation have been reported, this method is currently being used clinically in Japan. Thus we selected this method in this study. After 14 days of culture, $CD4^+$ cells were isolated using a magnetic-activated cell sorting (MACS) system (Miltenyi Biotec, Bergisch Gladbach, Germany) according to the manufacturer's instructions. As a control, mononuclear cells isolated from the peripheral blood of healthy volunteers were similar examined.

Polymerase chain reaction (PCR)

Total RNA was extracted from cells using an RNeasy kit (Qiagen, Valencia, CA) and reverse-transcribed using a First-Strand cDNA synthesis kit (GE Healthcare Bio-Science Corp., Little Chalfont, Buckinghamshire, UK) according to the manufacturer's instructions. Using cDNA synthesized from 150 ng of total RNA as a template for one amplification, real-time reverse transcriptase (RT)-PCR was performed using SYBR® Green PCR master mix, TaqMan® Universal PCR master mix and TaqMan® gene expression assays (Applied Biosystems, Foster City, CA), and an inventoried assay carried out on an ABI PRISM® 7900HT sequence detection system (Applied Biosystems) according to the instructions provided. Either the glyceraldehyde-3-phosphate dehydrogenase (GAPDH) gene or the β-actin gene was used as an internal control for normalization. The sequences of gene-specific primers for real-time RT-PCR are listed in Table 1.

DNA microarray analysis

The microarray analysis was performed as previously described.[9] Total RNA isolated from cells was reverse-

Table 1. The sequences of gene-specific primers for reverse transcriptase–polymerase chain reaction (RT-PCR) and real-time RT-PCR used in this study

Primer	Sequence
IL-4 forward	CACAGGCACAAGCAGCTGAT
IL-4 reverse	CCTTCACAGGACAGGAATTCAAG
IL-6 forward	GTAGCCGCCCCACACAGA
IL-6 reverse	CCGTCGAGGATGTACCGAAT
IL-10 forward	GCCAAGCCTTGTCTGAGATGA
IL-10 reverse	CTTGATGTCTGGGTCTTGGTTCT
IL-17 forward	GACTCCTGGGAAGACCTCATTG
IL-17 reverse	TGTGATTCCTGCCTTCACTATGG
IL-17F forward	GCTTGACATTGGCATCATCAA
IL-17F reverse	GGAGCGGCTCTCGATGTTAC
IL-23 forward	GAGCCTTCTCTGCTCCCTGATAG
IL-23 reverse	AGTTGGCTGAGGCCCAGTAG
IL-23R forward	AACAACAGCTCGGCTTTGGTATA
IL-23R reverse	GGGACATTCAGCAGTGCAGTAC
IFNG forward	CATCCAAGTGATGGCTGAACTG
IFNG reverse	TCGAAACAGCATCTGACTCCTTT
GM-CSF forward	CAGCCCTGGAGCATGTG
GM-CSF reverse	CATCTCAGCAGCAGTGTCTCTAC^{r}
RORγt forward	TGGGCATGTCCCGAGATG
RORγt reverse	GCAGGCTGTCCCTCTGCTT
STAT-3 forward	GGAGGAGGCATTCGGAAAGT
STAT-3 reverse	GCGCTACCTGGGTCAGCTT
FOXP3 forward	GAGAAGCTGAGTGCCATGCA
FOXP3 reverse	GCCACAGATGAAGCCTTGGT

IL, interleukin; *IFNG*, interferon γ; *FOXP3*, forkhead box protein 3; *GM-CSF*, granulocyte–macrophage colony-stimulating factor; *RORγt*, retinoic acid receptor-related orphan receptor γ isoform t; *STAT*, signal transducer and activator of transcription.

transcribed and labelled using One-Cycle Target Labeling and Control Reagents as instructed by the manufacturer (Affymetrix, Santa Clara, CA). The labelled probes were hybridized to a Human Genome U133 Plus 2·0 Array (Affymetrix). The arrays were used in a single experiment and analysed with GENECHIP operating software 1.2 (Affymetrix). Background subtraction and normalization were performed using GENESPRING GX 7.3 software (Agilent Technologies, Santa Clara, CA). The signal intensity was pre-normalized based on the positive control genes (GAPDH and β-actin) for all measurements on that chip. To account for differences in detection efficiency between spots, the pre-normalized signal intensity of each gene was normalized to the median of pre-normalized measurements for that gene. The data were filtered as follows. (i) Genes that were scored as absent in all samples were eliminated. (ii) Genes with a signal intensity of < 90 were eliminated. (iii) Genes that exhibited increased (fold-change > 2) or decreased (fold-change > 2) expression in CB-derived $CD4^+$ T cells compared with PB-derived $CD4^+$ T cells were selected by comparing the mean value of signal intensities in each condition.

Immunofluorescence study

After periods of cultivation, cells were collected and stained with fluorescence-labelled monoclonal antibodies and analysed by flow cytometry (FC500; Beckman/Coulter, Fullerton, CA). A four-colour immunofluorescence study was performed with a combination of fluorescein isothiocyanate (FITC)-conjugated anti-CD3, phycoerythrin (PE)-conjugated anti- forkhead box protein 3 (Foxp3), phycoerythrin-cyanine-5 (PC5)-conjugated anti-CD4 and PC7-conjugated anti-CD8 (Beckman/Coulter). After staining of cell surface antigens, cells were permeabilized with IntraPrep (Dako, Glostrup, Denmark) and intracellular antigen (Foxp3) was further stained.

Statistical analysis

The statistical analysis was performed using a Student's *t*-test and a *P*-value < 0·05 was considered to be statistically significant.

Results

Expression profiles of activated $CD4^+$ T cells derived from human CB and PB

To compare the gene expression patterns of CB-derived $CD4^+$ cells and PB-derived $CD4^+$ cells, we performed DNA microarray analysis using the Affymetrix Human Genome U133 Plus 2·0 Array. After background subtraction, comparison of the gene expression profiles of two independent CB-derived $CD4^+$ samples and PB-derived $CD4^+$ samples was performed using a gene cluster analysis. The genes differentially expressed (fold-change > 2) between the activated $CD4^+$ T cells derived from CB and those derived from PB were selected, and 396 probes were found to exhibit higher levels of expression in CB-derived $CD4^+$ samples while 131 probes exhibited higher levels in PB-derived $CD4^+$ samples. Parts of the data are summarized and presented in Fig. 1a and Tables 2–4.

Among these genes, those closely correlated to T-cell function and development were selected (Fig. 1b). The genes exhibiting higher levels of expression in CB-derived $CD4^+$ samples included those encoding cell cycle regulators, including cyclin-dependent kinase (CDKN)2A and 2B, transcriptional regulators and signal transduction factors (Tables 2 and 3). The genes for cytokines, chemokines and their receptors such as Interferon γ (IFNG), granulocyte-macrophage colony-stimulating factor (GM-CSF) and for T-cell transcriptional regulators (*FOXP3*) as well as the genes related to T-cell development including CD28, cytotoxic T lymphocyte antigen-4 (CTLA4) and inducible T-cell co-stimulator (ICOS) were also found among the genes exhibiting higher levels of expression in CB-derived $CD4^+$ samples (Fig. 1b). The factors reported

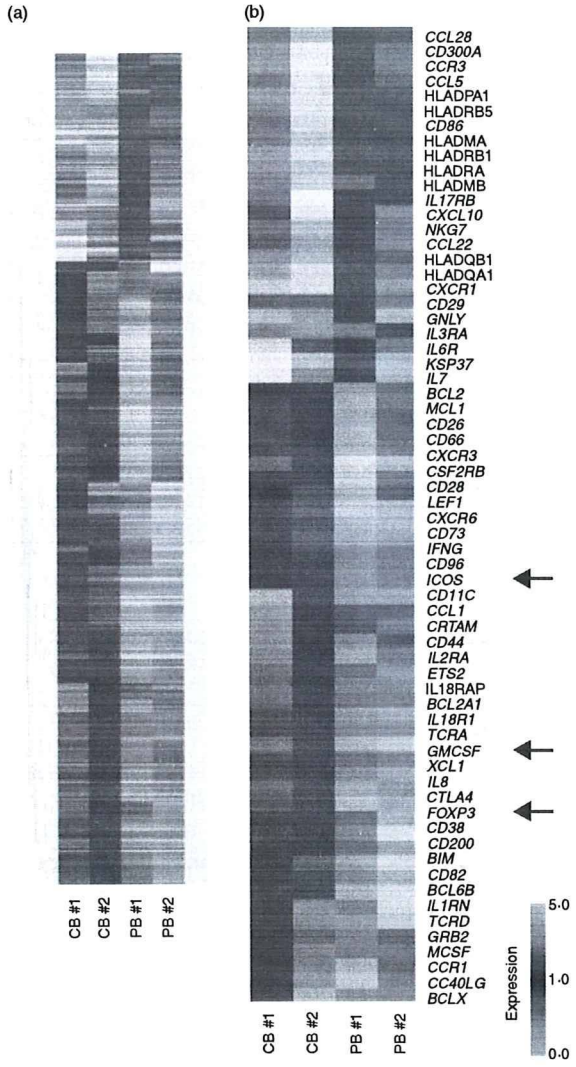

Figure 1. Comparison of the gene expression profiles of cord blood (CB)- and peripheral blood (PB)-derived $CD4^+$ T cells. Hierarchical clustering of results from a microarray analysis for CB- and PB-derived $CD4^+$ T cells is indicated. (a) A total of 529 genes characterizing $CD4^+$ T cells (396 genes for CB-derived $CD4^+$ T cells and 131 genes for PB-derived $CD4^+$ T cells) were used to create the gene tree. The gene list is presented in Tables 3 and 4. (b) Genes related to T-cell development (40 genes for CB-derived $CD4^+$ T cells and 26 genes for PB-derived $CD4^+$ T cells) are presented. The arrows indicate the expression pattern of T-cell lineage-specific genes including inducible T-cell co-stimulator (*ICOS*), granulocyte-macrophage colony-stimulating factor (*GM-CSF*) and forkhead box protein 3 (*FOXP3*).

to be essential for negative selection in $CD4^+$ $CD8^+$ thymocytes such as BCL2-like 11 (BIM)[10] as well as other apoptotic regulators were also found among the genes exhibiting higher expression levels in CB-derived $CD4^+$ samples.

The genes with a higher level of expression in the PB-derived $CD4^+$ T cells included those encoding transcriptional regulators, signal transduction factors, major histocompatibility complex (MHC) class II molecules (*HLADMA*, *HLADMB*, *HLADPA1*, *HLADQB1*, *HLADRA*, *HLADRB1* and *HLADRB5*), and cytokines, chemokines and their receptors (*IL-7*, *IL-17RB*), as well as genes that characterize the T-cell lineage (*CD29*, *CD86*) (Fig. 1b, Tables 2, 4).

Notably, microarray studies showed that the expression of several regulatory T cell (Treg)-related genes was significantly higher in the CB-derived T cells. Foxp3 is an important T-cell transcription factor and is considered to be a marker of Tregs. Cytotoxic T-lymphocyte antigen-4 (CTLA-4) and ICOS, which belong to the CD28 family of receptors and play a crucial role in the activation of T cells, were reported to be highly expressed in activated Tregs.[11,12] All of the above genes were expressed at higher levels in the CB-derived CD4 T cells (Fig. 1).

The microarray results for major genes related to the development of the T-cell lineage, including those not appeared in Fig. 1, are summarized in Table 2. As shown in Table 2, the expression of T-cell lineage master regulator genes, such as *TBX21*, *GATA3* and *MAF*, and T cell-related cytokines, such as *IL-4*, *IL-5*, *IL-13*, *IL-22* and *TGFB1*, revealed no significant difference between CB-derived $CD4^+$ cells and PB-derived $CD4^+$ cells. However, other T cell-related genes, including *IL-2*, *IL-6*, *IL-9*, *IL-10* and *IL-17*, were eliminated from the list in the course of background subtraction because the signal intensity of each gene was low (< 90 as raw data) in all of the samples.

Differences in the expression patterns of T-cell lineage-specific genes between CB-derived and PB-derived $CD4^+$ T cells

To further confirm the characteristic gene expression in CB- and PB-derived $CD4^+$ T cells, we performed a real-time RT-PCR analysis. Consistent with the microarray data, when the mRNA levels of the genes related to the T helper type 1 (Th1) and Th2 phenotypes were examined, higher levels of GM-CSF and IFNG were observed in CB-derived T cells, while IL-4 revealed no significant tendency (Fig. 2). We also examined IL-6 and IL-10 and no significant tendency was observed either in the expression of these genes (Fig. 2).

Next we examined the expression of the genes related to Tregs and observed a higher level of Foxp3, but lower levels of retinoic acid receptor-related orphan receptor γ isoform t (RORγt); and IL-17F, in CB-derived T cells (Fig. 3). In contrast, there was no significant tendency in the expression of genes encoding signal transducer and activator of transcription 3 (STAT-3), IL-23 and IL-23 receptors. In the case of the *IL-17* gene, clear amplifica-

Table 2. The microarray results for T-cell-related genes

Description	Gene	Gene ID	CB-1		CB-2		PB-1		PB-2	
			Normalized	Raw	Normalized	Raw	Normalized	Raw	Normalized	Raw
Master regulation										
Thl	*TBX21*	220684_at	1·1382915	305·7	0·7851455	247·1	1·045663	230·5	0·954337	261·4
Th2	*GATA3*	209602_s_at	1·471558	1204	0·7742825	742·1	1·0740323	721·1	0·9259675	772·5
	GATA3	209603_at	1·265932	416·5	0·53335179	205·7	1·0535141	284·5	0·9464856	317·6
	GATA3	209604_s_at	1·350573	5300	0·6415387	2950	1·0573606	3406	0·9426395	3773
	MAF	206363_at	0·7447395	672·7	0·8744312	925·6	1·1255689	834·5	1·2704437	1170
	MAF	209348_s_at	1·0320604	2078	0·8329663	1965	0·9679398	1600	1·8301903	3758
	MAF	229327_s_at	0·9099149	569·7	0·6089576	446·8	1·090085	560·2	1·4076804	898·9
Treg	*FOXP3*	221334_s_at	1·8893701	100·6	1·4199468	88·6	0·4988136	21·8	0·5800531	31·5
	FOXP3	224211_at	1·6205869	152·3	1·4101433	155·3	0·5898568	45·5	0·2347433	22·5
Cytokines										
Thl	*IFNG*	210354_at	1·4801383	2000	1·9182948	3037	0·457517	507·4	0·5198616	716·4
	GM-CSF	210229_s_at	1·2802086	1293	2·6726868	3163	0·6906437	572·5	0·7197912	741·4
Th2	*IL-4*	207538_at	2·0291064	687·2	0·3361219	133·4	0·9317174	259	1·0682826	369
	IL-4	207539_s_at	2·8263247	965	0·3561467	142·5	0·8481774	237·7	1·1518226	401·1
	IL-5	207952_at	1·3380713	810	0·0610382	43·3	1·0097023	501·7	0·9902797	611·4
	IL-13	207844_at	3·9835246	1712	0·8117443	408·8	1·1453367	404	0·8691162	452·9
Treg	*TGFB1*	203085_s_at	1·5166419	774·9	0·9012154	539·6	1·0987847	460·8	0·8546632	374·6
Others	*IL-22*	222974_at	0·1272062	5·2	4·325279	207·2	0·5632869	18·9	1·4367131	59·9
Surface molecules										
Treg	*CTLA4*	231794_at	1·3871489	536·9	1·2560804	357·5	0·7439196	148·3	0·4444751	110·1
	CTLA4	236341_at	1·2573498	905·7	1·6210791	1368	0·6800935	402·1	0·7426501	545·6
Others	*IL-2RA*	206341_at	1·5216751	3569	1·2715342	3494	0·7284654	1402	0·6569936	1571
	IL-2RA	211269_s_at	1·1563299	4436	1·3173387	5923	0·8436702	2657	0·560745	2194
	ICOS	210439_at	1·278036	619·8	1·343834	708·3	0·567216	209·4	0·656166	301
	CD28	211856_x_at	1·3887135	144·9	1·2905376	157·8	0·3292731	28·2	0·7094624	75·5
	CD28	211861_x_at	1·350062	183·3	1·4109998	224·5	0·4863549	54·2	0·649938	90

The microarray results for major genes related to the development of the T-cell lineage are summarized. The normalized and raw data for four samples are indicated for each gene. Those for which differential expression was found between cord blood (CB)- and peripheral blood (PB)-derived $CD4^+$ T cells in a gene cluster analysis (fold-change > 2) are highlighted in grey. Genes exhibiting low signal intensity (< 90 as raw data) in all of the four samples were eliminated from the list beforehand in the process of background subtraction, and thus do not appeared in this table.

CTLA-4, cytotoxic T-lymphocyte antigen-4; *FOXP3*, forkhead box protein 3; GATA, GATA family of zinc finger trancription factors; *GM-CSF*, granulocyte–macrophage colony-stimulating factor; ICOS, inducible T-cell co-stimulator; IFNG, interferon γ; *IL*, interleukin; MAF, macrophage-activating factor; TBX21, T-box protein 21; TGFB1, transforming growth factor, beta 1; Th1, T helper type 1; Treg, regulatory T cell.

tion was detected in PB-derived T cells whereas no amplification was observed in the samples of CB-derived T cells (data not shown).

To further investigate whether increased expression of the *FOXP3* gene is a general feature of CB-derived $CD4^+$ T cells, we tested four samples of CB-derived $CD4^+$ T cells by real-time RT-PCR analysis and compared the results with those for equivalent numbers of PB-derived samples. As shown in Fig. 4, two CB-derived samples (CB 4 and 5, at 2 weeks) revealed significantly increased gene expression of *FOXP3* when compared with PB-derived samples, whereas the remaining two samples (CB 3 and 6; termed 'additional' samples below) did not. We also tested *FOXP3* gene expression at an earlier time-point in the same samples and observed no significant increase of *FOXP3* gene expression in CB-derived $CD4^+$ T cells at 1 week (Fig. 4). When the data were analysed statistically, expression of the *FOXP3* gene was found to be significantly higher in CB-derived $CD4^+$ T cells in comparison with equivalent PB-derived $CD4^+$ T cells at both 1 week ($P < 0{\cdot}05$) and 2 weeks ($P < 0{\cdot}05$) (Fig. 4).

Next we assessed the expression of the Foxp3 protein in CB-derived $CD4^+$ T cells. When the same samples as described above were examined by flow cytometry using a specific antibody, the Foxp3 protein was certainly detected in a portion of cells in all of four CB-derived samples while not detected in any of the PB-derived samples tested (Fig. 5). Inconsistent with the results of real-time RT-PCR, expression level of Foxp3 proteins was higher in CB-derived $CD4^+$ T cells at 1 week than at 2 weeks.

Table 3. Genes up-regulated in $CD4^+$ T cells from cord blood samples 1 and 2 (CB 1 and CB 2, respectively)

		Fold change				
Affi ID	Gene abbreviation	CB 1	CB 2	PB 1	PB 2	Gene name
Apoptosis						
1555372_at	*BimL*	1·39	1·52	0·61	0·42	BCL2-like 11 (apoptosis facilitator)
237837_at	*BCL2*	1·27	1·32	0·49	0·73	B-cell CLL/lymphoma 2
205681_at	*BCL2A1*	1·91	1·53	0·39	0·47	BCL2-related protein A1
1558143_a_at	*BCL2L11*	1·68	1·74	0·32	0·32	BGL2-like 11 (apoptosis facilitator)
228311_at	*BCL6B*	1·36	3·39	0·64	0·26	B-cell CLL/lymphoma 6, member B (zinc finger protein)
215037_s_at	*BCLX*	2·56	1·27	0·73	0·56	BCL2-like 1
224414_s_at	*CARD6*	2·65	1·34	0·56	0·66	Caspase recruitment domain family, member 6
201631_s_at	*IER3*	1·62	2·95	0·38	0·31	Immediate early response 3
218000_s_at	*PHLDA1*	2·34	1·21	0·53	0·79	Pleckstrin homology-like domain, family A, member 1
209803_s_at	*PHLDA2*	2·87	1·32	0·31	0·68	Pleckstrin homology-like domain, family A. member 2
203063_at	*PPMIF*	1·26	1·53	0·74	0·64	Protein phosphatase IF (PP2C domain containing)
205214_at	*STK17B*	1·78	1·26	0·74	0·71	Serine/threonine kinase 17b (apoptosis-inducing)
217853_at	*TENS1*	1·63	6·00	0·04	0·37	Tensin 1
B- and T-cell development						
211861_x_at	*CD28*	1·35	1·41	0·49	0·65	CD28 antigen(Tp44)
207892_at	*CD40LG*	3·67	1·32	0·45	0·68	C040 ligand (TNF superfamily, member 5, hyper-IgM syndrome)
206914_at	*CRTAM*	2·76	1·60	0·40	0·36	Class I MHC-restricted T-cell-associated molecule
210557_x_at	*CSF1*	3·79	1·22	0·78	0·70	Colony-stimulating factor 1 (macrophage)
210229_s_at	*CSF2*	1·28	2·67	0·69	0·72	Colony-stimulating factor 2 (granulocyte–macrophage)
205159_at	*CSF2RB*	2·33	1·60	0·18	0·40	Colony-stimulating factor 2 receptor
231794_at	*CTLA4*	1·39	1·26	0·74	0·44	Cytotoxic T-lymphocyte-associated protein 4
204232_at	*FCER1G*	1·63	2·14	0·28	0·37	Fc fragment of IgE, high affinity 1, receptor for; gamma polypeptide
210439_at	*ICOS*	1·38	1·34	0·57	0·66	Inducible T-cell costimulator
210354_at	*IFNG*	1·48	1·92	0·46	0·52	Human mRNA for HuIFN -gamma interferon
230536_at	*PBX4*	1·48	1·26	0·50	0·74	Pre-B-cell leukaemia transcription factor 4
215540_at	*TCRA*	1·25	1·87	0·67	0·75	T-cell antigen receptor alpha
234440_al	*TCRD*	7·51	1·48	0·50	0·52	Human T-cell receptor delta-chain
Cell growth and maintenance						
213497_at	*ABTB2*	2·06	1·34	0·66	0·63	Ankyrin repeat and BTB (POZ) domain containing 2
201236_s_at	*BTG2*	1·60	1·23	0·60	0·77	BTG family, member 2
235287_at	*CDK6*	1·50	1·32	0·44	0·68	Cyclin-dependent kinase 6
209644_x_at	*CDKN2A*	2·90	1·21	0·67	0·79	Cyclin-dependent kinase inhibitor 2A (melanoma, p16, inhibits CDK4)
236313_at	*CDKN2B*	3·24	1·28	0·58	0·72	Cyclin-dependent kinase inhibitor 2B (p15, inhibits CDK4)
241984_at	*CHES1*	1·38	1·34	0·66	0·63	Checkpoint suppressor 1
202552_s_at	CRIM1	1·94	1·39	0·32	0·61	Cysteine-rich transmembrane BMP regulator 1 (chordin-like)
204844_at	*ENPEP*	1·64	1·75	0·09	0·36	Glutamyl aminopeptidase (aminopeptidase A)
205418_at	*FES*	1·39	1·80	0·61	0·25	Feline sarcoma oncogene
228572_at	*GRB2*	4·69	1·21	0·79	0·78	Growth factor receptor-bound protein 2
207688_s_at	*INHBC*	1·46	1·25	0·51	0·75	Inhibin, beta C
209744_x_at	*ITCH*	1·30	1·47	0·63	0·70	Itchy homolog E3 ubiquitin protein ligase (mouse)
201548_s_at	*JARID1B*	1·27	1·92	0·73	0·46	Jumonji, AT-rich interactive domain IB (RBP2-like)
203297_s_at	*JARID2*	1·42	1·28	0·54	0·72	Jumonji, AT-rich interactive domain 2
41387_r_at	*JMJD3*	1·82	1·24	0·76	0·65	Jumonji domain containing 3
205569_at	*LAMP3*	2·32	1·24	0·76	0·50	Lysosomal-associated membrane protein 3
214039_s_at	*LAPTM4B*	1·41	1·49	0·49	0·59	Lysosomal-associated protein transmembrane 4 beta
205857_x_at	*MSH3*	1·79	1·28	0·58	0·72	MutS homolog 3 (*E. coli*)
209550_at	*NDN*	3·42	1·38	0·17	0·62	Necdin homolog (mouse)
207943_x_at	*PLAGL1*	1·37	1·43	0·57	0·63	Pleiomorphic adenoma gene-like 1
204748_at	*PTGS2*	1·65	1·78	0·14	0·35	Prostaglandin-endoperoxide synthase 2
201482_at	*QSCN6*	1·32	1·23	0·38	0·77	Quiescin Q6
203743_s_at	*TDG*	1·47	1·23	0·54	0·77	Thymine-DNA glycosylase
204227_s_at	*TK2*	2·12	1·26	0·56	0·74	Thymidine kinase 2, mitochondrial

